



HAL
open science

Mid- to Late-Holocene coastal morphological evolution, vegetation history and land-use changes of the Porto Gulf UNESCO World Heritage site and its surroundings (NW Corsica Island, Western Mediterranean)

Matthieu Ghilardi, Jordi Revelles, Jean-Baptiste Mary, Federico Di Rita,
Claire Delhon, Sébastien Robresco

► To cite this version:

Matthieu Ghilardi, Jordi Revelles, Jean-Baptiste Mary, Federico Di Rita, Claire Delhon, et al.. Mid- to Late-Holocene coastal morphological evolution, vegetation history and land-use changes of the Porto Gulf UNESCO World Heritage site and its surroundings (NW Corsica Island, Western Mediterranean). *The Holocene*, 2023, 33 (9), pp.1023-1044. 10.1177/09596836231176492 . hal-04116323

HAL Id: hal-04116323

<https://hal.science/hal-04116323>

Submitted on 5 Jun 2023

HAL is a multi-disciplinary open access archive for the deposit and dissemination of scientific research documents, whether they are published or not. The documents may come from teaching and research institutions in France or abroad, or from public or private research centers.

L'archive ouverte pluridisciplinaire **HAL**, est destinée au dépôt et à la diffusion de documents scientifiques de niveau recherche, publiés ou non, émanant des établissements d'enseignement et de recherche français ou étrangers, des laboratoires publics ou privés.

1
2
3 1 **Mid- to Late Holocene coastal morphological evolution, vegetation history and land-use changes of**
4 2 **the Porto Gulf UNESCO World Heritage site and its surroundings (NW Corsica Island, Western**
5 3 **Mediterranean)**
6
7
8

9 5 **Matthieu Ghilardi¹, Jordi Revelles^{2,3}, Jean-Baptiste Mary⁴, Federico Di Rita⁵, Claire Delhon⁶, Doriane**
10 6 **Delanghe¹, Sébastien Robresco⁷**

11 7 **Abstract**

12 8 Two coastal areas located on the North-Western side of Corsica Island have been investigated to
13 9 reconstruct their Mid- to Late Holocene landscape evolution together with the history of human
14 10 occupation. Particular attention has been paid to the study of shoreline migration and vegetation
15 11 history alongside land-use. Three boreholes were drilled to a maximum depth of 4.20 m and laboratory
16 12 work comprised the identification of molluscs and pollen/NPPs as well as sedimentological analyses.
17 13 Chronostratigraphy is based on a series of 18 radiocarbon datings and enabled to reconstruct the
18 14 environments in the Fangu Estuary to the north of the World Heritage site over the last six millennia,
19 15 and over the last four millennia on the Girolata coastal plain to the south. Palaeogeographic
20 16 reconstructions of shoreline mobility are established for each site based on borehole
21 17 chronostratigraphy analysis. In addition, two original pollen and NPPs diagrams were established for
22 18 the Girolata and Fangu sites. These reveal that anthropogenic activities began to significantly impact
23 19 local vegetation cover ca. 2500 years BP at Girolata, and ca. 2000 years BP at Fangu. Of particular
24 20 interest, our work records the first complete pollen sequence in Corsica for Roman times at Girolata:
25 21 first, the exploitation of cereals, grapevines and the development of husbandry is observed during the
26 22 Roman Republic (500 BCE-0), followed by the almost exclusive cultivation of *Olea* sp. during the Roman
27 23 Empire (0-500 CE). Following this, and using other regional pollen studies obtained for NW Corsica, we
28 24 propose a regional evolution of the complex human-environment interactions for the last six millennia.
29 25 Our results reveal a peak of regional forest decline (the most intense event recorded for the Late
30 26 Holocene) from the 11th to the 16th centuries CE which can be attributed to the exploitation of wood
31 27 resources during the Pisan and Genoese dominations of the island.
32 28

33 29 **Keywords : Palaeoenvironments, Vegetation history, land-use, UNESCO World heritage site, Coastal**
34 30 **landscape, Corsica**
35 31
36 32
37 33

38 34 1. Introduction

39 35 The coastal wetlands of the Mediterranean are of particular interest when reconstructing short- to
40 36 long-term human-environment interactions, mainly at a local scale, as is attested by the abundant
41 37
42 38
43 39
44 40
45 41
46 42
47 43
48 44
49 45
50 46
51 47
52 48
53 49
54 50
55 51
56 52
57 53
58 54
59 55
60 56

51 ¹CEREGE – AMU-CNRS-IRD-Collège de France-INRAE, Europôle de l'Arbois BP 80 13545 Aix-en-Provence CEDEX 04, France.
52 matthieu.ghilardi@cnrs.fr

53 ²Institut Català de Paleocologia Humana i Evolució Social (IPHES-CERCA), Zona Educacional 4, Campus Sescelades URV (Edifici
54 W3), 43007 Tarragona, Spain.

55 ³Universitat Rovira i Virgili, Departament d'Història i Història de l'Art, Avinguda de Catalunya 35, 43002 Tarragona,
56 Spain

57 ⁴University of Lyon 2, Hisoma, Collectivité de Corse

58 ⁵University of Roma La Sapienza

59 ⁶University of Nice – CEPAM CNRS

60 ⁷SIGOSPHERE, Chazay d'Azergues, France

1
2
3
4
5
6
7
8
9
10
11
12
13
14
15
16
17
18
19
20
21
22
23
24
25
26
27
28
29
30
31
32
33
34
35
36
37
38
39
40
41
42
43
44
45
46
47
48
49
50
51
52
53
54
55
56
57
58
59
60

literature treating this topic over the last decade (Di Rita and Magri, 2012; Fontana et al., 2017; Melis et al., 2017; Poher et al., 2017; Brisset et al., 2018; Pascucci et al., 2018; Marco-Barba et al., 2019; Revelles et al., 2019). The general calm conditions accompanying sediment vertical accretion allow the acquisition of continuous sedimentary series, making coastal wetlands suitable places to reconstruct Early- to Late Holocene environmental changes, using a series of sedimentological, geochemical and palaeoecological proxies (Sabatier et al., 2010; Marco-Barba et al., 2013; Brisset et al., 2018; Lopez-Belzunce et al., 2020; Giaime et al., 2022). Along Corsica's shoreline (~1050 km long) where human occupation is well attested and documented, two hundred brackish (mostly lagoons and swamps) to freshwater ponds are found (Ghilardi, 2020 and 2021). These latter could potentially be cored in order to improve our understanding of landscape configuration over the last six to eight millennia. Indeed, over the last decade, Corsica, the fourth largest Mediterranean island (area of ca. 8720 km²), has been studied in an attempt to reconstruct human-environment interplays with robust chronostratigraphies on the coastal zone (Currás et al., 2017; Ghilardi et al., 2017a; Revelles et al., 2019; Vella et al., 2019; Di Rita et al., 2022a). All these studies are based on pollen analyses and have focused on human-environment interactions since Neolithic times (Currás et al., 2017; Ghilardi et al., 2017a; Poher et al., 2017; Revelles et al., 2019; Vella et al., 2019; Di Rita et al., 2022a). Some of these studies have also revealed that most of the coastal plains formed during the Late Holocene due to a general mechanism of deltaic progradation of the river mouths (Currás et al., 2017; Ghilardi et al., 2017a) following a period of maximum sea incursion that can be dated slightly before the Mid-Holocene (Vacchi et al., 2016 and 2018; Revelles et al., 2019). The Porto Gulf UNESCO World Heritage site (listed in 1983) in NW Corsica covers an area of ca. 120 km² that includes the Girolata Gulf, the Scandola Peninsula and the Fangu River (Figure 1), where a small number of coastal wetlands can be identified on the coastal plains. Until now, no geoarchaeological studies have attempted to reconstruct the human-environment interplays during the Holocene for the entire UNESCO site. However, extensive archaeological surveys conducted since the mid- 2010s attest to the presence of humans over the last ca. 2500 years at least, corresponding to the Roman (Cibecchini and Dieulefet, 2014) and Medieval periods (Huser et al., 2017; Mary, 2021 and 2022). Nonetheless, there are few known remains that reveal the complete history of the human occupation and land-use practices during Protohistory, Antiquity, and the Middle Ages. Based on archaeological findings, the Girolata and Fangu coastal plains may possibly have served as natural harbours (protected bays) since Early Roman times when the seashore was probably located further inland. In order to elucidate these geoarchaeological questions and to locally reconstruct past morphological changes and vegetation dynamics as well as land-use, the two main coastal areas (Girolata Plain and Fangu Estuary) were investigated. The aim of the present paper is to provide additional pollen sequences in the NW area of Corsica in order to obtain a full view of the vegetation history at the regional scale and over the last millennia, as influenced by human activities and other factors determining landscape changes, in particular during Protohistory, Roman and medieval times.

2. Site presentation and archaeological settings

2.1. The Girolata Plain

2.1.1. Topography and geology of the area

The Girolata Plain is situated south of the Scandola nature reserve (Figure 1) and covers an area of ca. 4 ha. Until recently, swamplands were present in the westernmost part of the plain which is drained by two intermittent streams: Girolata Stream (Fig. 2A) to the east and Novalla Stream (Fig. 2A) to the west. Both rivers drain primarily Upper Carboniferous/Lower Permian rhyodacitic rocks of volcanic origin in the upper part of the drainage basins, and monzogranite in the lowermost part of the river valleys (Vellutini et al., 1985 and 1996; Huser et al., 2017; Figure 2A). Locally, Palaeozoic micaschists

1
2
3 85 outcrops are identified to the west of the catchment (Figure 2A). The Girolata coastal plain is limited
4 86 to the South East by a coastal barrier formed by well-rounded pebbles embedded within a matrix of
5 87 gravels and coarse sands, turning the flat plain into a back-ridge depression (Figure 2B).
6 88

8 89 2.2.2. Previous geomorphological studies

9 90 In the late 2010s, geomorphological investigations (Huser et al., 2017) carried out in the north-eastern
10 91 part of the Girolata Plain revealed a succession of different environments, starting from marine to
11 92 shallow marine during the Middle Bronze Age (1800-1350 BCE), followed by mainly terrestrial
12 93 environments, potentially dated after Antiquity. However, the rather low number of sedimentary
13 94 sequences obtained and dated by only two radiocarbon datings were insufficient to enable a full
14 95 reconstruction of the palaeogeography of the plain over the last four millennia. In addition, no
15 96 information concerning past land-use and human-environment interactions was gained for this period.
16 97

18 98 2.2.3. Archaeological settings

19 99 There are no trace remains of human occupation for the Prehistoric and Protohistoric periods
20 100 throughout the catchment areas of Novalla and Girolata Streams nor in the vicinity of the Girolata
21 101 Plain. For the subsequent cultural periods, recent archaeological surveys have revealed an important
22 102 phase of human occupation during Roman times, ranging from the late 3rd century BCE until the early
23 103 7th century CE (Cibecchini and Dieulefet, 2014; Mary, 2014a; 2014b; 2014c; 2018; 2021 and 2022; Huser
24 104 et al., 2017). The site of Chjesaccia, located on a smooth granitic outcrop and situated a short distance
25 105 from the present day shoreline of the Girolata Plain (Figs. 2A and 2B) yielded important findings. This
26 106 site is also situated a very short distance from the stratigraphic profile studied in 2017 (Huser et al.,
27 107 2017). In particular, tegulae (flat roofing tiles) and different building structures (apses) have been
28 108 discovered and can probably be associated to an important coastal site dating roughly from the 3rd
29 109 century BCE to the 2nd to 3rd centuries CE (Mary, 2014a, 2014b, 2020). Recent archaeological
30 110 excavations have revealed a building probably dated from the 1st century CE (Mary, 2020) located to
31 111 the west of the plain, in the modern village of Girolata. Beyond the coastal plain and its immediate
32 112 surroundings, the Novalla River valley evidences (surface surveys) the presence of material dated from
33 113 the 2nd and 3rd centuries CE at two sites (Figure 2A) named Novalla (mid- main stream) and Calanchelle
34 114 (upper stream; Mary, 2014a, 2014b).

35 115 Traces of modern nautical activity have been dated to the 16th-18th centuries CE (Cibecchini and
36 116 Dieulefet, 2014) and remarkable buildings located primarily in the westernmost part of the Girolata
37 117 Plain have been identified. The aim of these structures was both to protect the coastline from invaders
38 118 (mainly the Ottomans, following the fall of Constantinople in 1453 CE) and to aid the development of
39 119 agriculture. The configuration of Girolata Bay offers a protected coastline that may have served as a
40 120 natural harbour. The construction of the nearby Girolata fort during the Genoese administration of the
41 121 island is certainly related to the presence of such a harbour, as is revealed by recent submarine surveys
42 122 (Cibecchini and Dieulefet, 2014).

43 123 The continuous occupation of the Girolata area over approximately two millennia (from the 3rd century
44 124 BCE until the 18th century CE) confirms the important geostrategic position of the protected Bay on the
45 125 western coast of the island and its role as a layover on the western Mediterranean maritime routes.
46 126

54 127 55 128 56 129 2.2. The Fangu coastal plain

57 130 58 131 2.2.1. Present-day topography and geology of the surroundings

59
60

1
2
3 32 The Fangu drainage basin covers an area of ca. 235 km² for a length of 24 km (Figure 1) and marks the
4 133 northern limit of both the UNESCO world heritage site and the Corsican regional park. The catchment
5 134 topography is characterised by steep slopes, with upper reaches situated at an elevation of 2335 m
6 135 amsl (Capu Tafunatu; Figure 1) with the highest summit culminating at 2556 m (Punta Minuta; Figure
7 136 1). The geology of the drainage basin can be divided into four main groups (Vellutini et al., 1985 and
8 137 1996): 1/ the metamorphic and sedimentary complex which is located on the northern bank of the
9 138 lower Fangu River valley. This complex dates from the Palaeozoic and is older than the volcanic
10 139 complex of Monte Cintu (Vellutini et al., 1985 and 1996). The metamorphic complex includes pre-
11 140 Devonian shales and schists (Figure 3A) while the sedimentary complex is made up of conglomerates
12 141 and sandstones dating to the Devonian (Figure 3A); 2/ the volcanic complex of Monte Cintu dates from
13 142 the onset of the Permian and composes half of the geology of the Fangu catchment. This complex
14 143 consists of rhyolites of different colours (Figure 3A); 3/ To the east, rhyolites with ignimbritic facies
15 144 form the eastern limit of the catchment where the higher summits are situated; 4/ The lower river
16 145 valley is characterised by an abundant alluvial sedimentation due to multiple migrations of the Fangu
17 146 River main course during the Quaternary. The river mouth does not connect with the sea at any time
18 147 of the year but forms a large coastal swamp, situated in the former river estuary behind a thick and
19 148 wide coastal barrier (Figure 3B), itself composed of rounded pebbles and a matrix of sands and gravels.
20
21
22
23
24

25 150 2.2.2. Archaeological settings

26 151 Human occupation of the area remains largely unknown due to the paucity of archaeological surveys
27 152 conducted. However, the modern period is well represented with the identification of two towers built
28 153 during the Genoese administration of the island. The first one was built in 1541 (Figs 3A and 3B) while
29 154 the second was built in the same location in 1574. The construction of these towers supports the
30 155 strategic position of the Fangu Estuary which, like Girolata Bay, probably served as a natural harbour
31 156 on the road from Calvi to Girolata on the north-western coast of Corsica. Forest exploitation can be
32 157 related to this coastal settlement, where wood trunks were transported from the uplands of the Fangu
33 158 drainage basin to the estuary before being loaded onto boats. Sawmills located at Pozzona on the
34 159 lower Fangu River were active between 1596 and 1608 CE (Graziani, 2004), and confirm this forest
35 160 activity. Other than this, little is known in terms of human presence, in particular during Roman times.
36 161 Many unanswered geoarchaeological questions remain concerning land use in the area, possibly linked
37 162 to the Girolata sector.
38
39
40

41 163 42 164 3. Methods

43 165 44 166 3.1. Core sampling

45 167 Three 50-mm diameter vibracores were drilled reaching a maximum depth of 4.20 m (Figs. 2A, 2B, 3A
46 168 and 3B). Each borehole was precisely mapped and subsequently levelled with topographic information
47 169 derived from a LIDAR survey (Table 1).
48
49
50

51 170 52 171 3.2. Grain-size analyses

53 172 Samples were taken at 5 cm intervals. Many samples exhibited coarse particles (gravels to pebbles)
54 173 above 2 mm. Wet-sieving by hand was then used to isolate the total fractions of coarse (>2 mm) and
55 174 fine sediments (<2 mm). For the layers which contained fine particles only (less than 2 mm), laser
56 175 diffraction grain-size analyses were undertaken. The grain-size distribution was measured using a
57 176 Beckman Coulter LS 13 320 laser granulometer with a range of 0.04 to 2000 µm, in 116 fractions
58 177 detected from 132 detectors (126 detectors for the scattering pattern and 6 detectors for the PIDS
59
60

1
2
3 78 (Polarization Intensity Differential Scattering) technology which is sensitive to sub-micron sized
4 179 particles). The calculation model (software version 5.01) uses the Fraunhofer and Mie theory. For the
5 180 calculation model we used water as the medium (RI = 1.33 at 20 °C) and a refractive index in the range
6 181 of that of kaolinite for the solid phase (RI = 1.56; Buurman et al., 1996). Samples containing fine
7 182 particles were diluted, enabling to measure between 8 and 12% of obscuration and between 45 and
8 183 70% PIDS obscuration.
9
10
11 184

12 185 3.3. Organic matter/carbonate content

13 186 Loss-on-ignition (LOI) measurements were conducted at CEREGE on cores Girolata 2 and Fangu
14 187 following Dean (1974) and Bengtsson and Enell (1986). Sediment samples of approximately 10 to 20 g
15 188 were taken at 5 cm intervals throughout the sequences. After drying at 105°C to constant weight, the
16 189 samples were heated to 550°C for 7 h to estimate the organic content. A second heating phase to
17 190 950°C for a further 7 h was undertaken to assess the proportion of carbonate.
18
19
20 191

21 192 3.4. AMS dating

22 193 The chronostratigraphy of the cores was established using a series of 18 AMS radiocarbon
23 194 determinations from charcoal, organic matter and plant remains (*Posidonia oceanica*) (Table 2). The
24 195 analyses were conducted in the Poznan (Poland) Radiocarbon Dating Laboratory. ¹⁴C ages were
25 196 calibrated using Calib Software Version 8.2 (Stuiver and Reimer, 1993) and the IntCal20 calibration
26 197 curve for terrestrial samples (Reimer et al., 2020). Marine samples (*Posidonia oceanica*) were corrected
27 198 for the local marine reservoir effect according to Siani et al. (2000) and Reimer and McCormac (2002)
28 199 where regional ΔR is -109 (± 40) in the area of Bastia (situated 75 km east of the study area). Finally,
29 200 the age-depth models were built in Clam.r 2.2. (Blaauw, 2010) using best fitting methods, smoothing
30 201 spline for Fangu and linear interpolation for Girolata 2 (Figure 4).
31
32
33
34
35 202

36 203 3.5. Mollusc identification

37 204 Cores Girolata 1, Elbu and Fangu were devoid of molluscs, while Girolata 2 was rich in fossils. All
38 205 samples were wet-sieved through a wire screen (0.40 mm mesh) and air dried at room temperature.
39 206 The residue was examined under a binocular microscope (magnification: $\times 10$) and all identifiable shells
40 207 and characteristic fragments were selected and placed in separate plastic tubes. Based on the
41 208 molluscan classification system which assigns Mediterranean species to well-defined ecological groups
42 209 (Péres and Picard, 1964; Péres, 1982), bio-sedimentary units were then established for the present
43 210 study.
44
45
46 211

47 212 3.6. Pollen identification

48 213 Pollen analysis was focused on 20 samples from the shallow marine sequence of the Girolata 2 core
49 214 and 24 from the Fangu core.

50 215 All (44) samples were processed following standard methods (Goeury and Beaulieu, 1979; Girard and
51 216 Renault-Miskovsky, 1969) using treatment with HCL, NaOH, flotation in dense Thoulet liquor, HF and
52 217 final mounting in glycerine. Around 300-350 pollen grains of terrestrial taxa were counted using an
53 218 Olympus Bx43 microscope fitted with $\times 10$ ocular lenses and $\times 40/60$ objectives. Hygrophyte and aquatic
54 219 plants (Cyperaceae, *Typha/Sparganium*, *Myriophyllum*, Ranunculaceae) and Amaranthaceae-
55 220 Chenopodioidae were excluded from the pollen sum to avoid over-representation by local taxa. All
56 221 pollen types are defined according to Reille (1992b). Cerealia-type was defined according to the
57
58
59
60

22 morphometric criteria of Faegri and Iversen (1989) (>40 µm pollen grain, >8 µm pore). *Alnus* spp. refers
223 to some alder species, in particular *Alnus glutinosa* and *Alnus alnobetula* var. *suaveolens* (Req.) Regel.
224 Non-pollen palynomorphs (NPP) identification followed van Geel (1978, 2001), van Geel et al. (2003),
225 Revelles et al. (2016) and Revelles and Van Geel (2016). A percentage pollen diagram was created using
226 Tilia software (Grimm, 1991-2011), and pollen zonation was defined using CONISS (Grimm, 1987); NPPs
227 are described in the context of the pollen zones.

229 4. Results

230 4.1. General stratigraphy

232 4.1.1. Girolata 1 core

233 This core is 3.15 m long and is characterized by the presence of very coarse material, mainly gravels
234 and pebbles along most the sequence. However, four sedimentary units can be distinguished (Figure
235 5):

236 - Sedimentary Unit 1 is found between 3.15 and 1.30 m deep and is characterized by an
237 alternation between layers of grey sands containing balls of the Mediterranean seagrass *Posidonia*
238 *oceanica* (depths of 2.95, 2.80, 1.92, 1.89, 1.82 and 1.66 m) and layers composed of gravels and a
239 mixture of well-rounded and angular pebbles of dacites/rhyodacites. Unit 1 contains no molluscs, and
240 with the exception of the layers containing *Posidonia oceanica*, the organic matter content is poor.
241 Two radiocarbon datings were performed on fibers of *Posidonia oceanica* : in the lowermost part of
242 Unit 1, at a depth of 2.96 m, an age of 1424-1047 cal. BCE was obtained, while in the uppermost part
243 of the unit, at a depth of 1.66 m, an age of 1317-917 cal. BCE was recorded. Unit 1 is characteristic of
244 marine environments with high energy of deposition, possibly in the supra tidal zone since no molluscs
245 or shell debris were found. It is noteworthy that the lithology of the detrital material composed of
246 gravels and pebbles is exclusively composed of dacites, the dominant rock of the Girolata catchment
247 (Fig. 2).

248 - Sedimentary Unit 2 is identified from 1.30 to 0.80 m and its deposition began roughly in the
249 early 1st millennium BCE, based on the radiocarbon dating results obtained for the top of the
250 underlying Unit 1. Sedimentological features clearly exhibit a generally calm environment of deposition
251 (clays), such as a coastal wetland where frequent terrestrial inputs are observed. The texture is a
252 mixture of coarse materials, mainly gravels and angular pebbles (dacites), deposited within a
253 sandy/clayey matrix. The lack of marine fauna and organic remains such as fibers of *Posidonia*
254 *oceanica* may reflect a full terrestrial sedimentation rather than a marine origin of deposition inside
255 the wetland.

256 - Sedimentary Unit 3 is found from 0.80 to 0.38 m. It consists of black organic clays with
257 abundant organic remains and sharp pebbles of dacyte within the clayey matrix, thus indicating local
258 detrital input into a swampland.

259 - Sedimentary Unit 4 is found between 0.38 m and the present day surface topography. It is
260 composed of light orange to brown silts indicative of the modern soil plough.

261 Any palaeoecological (pollen based vegetation reconstruction) interest in these sedimentary units
262 appeared to be very limited and was therefore not studied.

265 4.1.2. Girolata 2 core

1
2
3 267 This core is 4.20 m long and encompasses the last 4.2 kyr according to chronostratigraphy based on
4 268 the radiocarbon dating results (Table 2). Five main biosedimentary units (Figure 6) can be defined from
5 269 the bottom to the top, as follows:

7 270 - Unit I is found between 4.20 and 2.95 m in depth and contains both marine molluscs and an
8 271 abundance of fibers of *Posidonia oceanica*. This sedimentary unit is composed of silty clays and fine
9 272 sands with mean grain size generally ranging between 50 and 150 μm . Organic matter content is
10 273 around 10 to 20%. The mollusc identification reveals strong representation of two main species:
11 274 *Bittium reticulatum* (a marine gastropod) and *Loripes lacteus* (a shallow marine bivalve that lives on a
12 275 sandy substratum), as well as *Cerastoderma glaucum*, *Clelandella miliaris*, *Tricolia pullus* and *Rissoa*
13 276 *ventricosa* (not exceeding 5% in total). The mollusc assemblage clearly indicates the presence of a
14 277 marine- to shallow marine environment dominated by a sandy sea bottom with development of the
15 278 typical seagrass *P. oceanica*. It is noteworthy that this unit contains well preserved and identifiable
16 279 pollen grains (see section 5.2.1). Radiocarbon dating was performed on the lowermost part of Unit I
17 280 and reveals an age of 1921-1696 cal. BCE at a depth of 4.1 m. Towards the top of the unit at a depth
18 281 of 3 m below the surface, an age of 1447-1286 cal. BCE was obtained. The above-described
19 282 palaeoenvironmental proxies help to identify Unit I as a marine- to shallow marine environment
20 283 (protected bay) with a sandy sea floor associated with calm dynamics of sedimentation. However, at
21 284 the top of the unit, from 3.10 to 3 m deep, a thin layer of black organic sandy clays containing shell
22 285 debris and some intact small specimens (juvenile) of *Bittium reticulatum* together with rare and intact
23 286 *Cerastoderma glaucum* bivalves (of centimetric size) can be found. Also observed embedded within
24 287 the clayey fraction were *P. oceanica* fibers. The top of Unit I (dated 1447-1286 cal. BCE) exhibits a clear
25 288 transition to a more confined environment, still connected with the sea, and appears to correspond to
26 289 a short phase of lagoonal development with very low energy of deposition.

31 290 - Unit II overlies Unit I and is found from 3 to 1.50 m below the surface. In general, it is composed
32 291 of coarse material made up of sharp pebbles (dacites), angular gravels and medium to coarse sands.
33 292 The radiocarbon dating performed at its transitions with Units I (below) and III (above) reveals that
34 293 Unit II was deposited from ca. 1447-1286 cal. BCE to 650 cal. BCE, according to the estimation of the
35 294 depth/age profile for this latter date. However, two sub-units can be distinguished and are described
36 295 as follows: Unit IIA consists of grey medium to coarse sands with rare small fragments of marine
37 296 molluscs (*Bittium reticulatum*) in its lowermost part. Several layers containing fibers of *Posidonia*
38 297 *oceanica* are identified at the depths of 2.66, 2.55 and 2.20m: these fibers are abundant in the
39 298 lowermost part of the unit. Unit IIB extends from 2.85 to 2.57 m and is composed of two layers of
40 299 orange to red oxidized coarse sands (mean grain size ca. 400-600 μm) and sharp gravels, separated
41 300 only by a thin layer (10 cm) of *Posidonia oceanica* and pebbles of dacite, dated to 1119-769 cal. BCE.
42 301 No molluscs were identified in either of Unit IIB's oxidized layers, which may be indicative of terrestrial
43 302 dynamics of deposition. In general, sedimentological results exhibit a higher energy of deposition in
44 303 Unit II than in Unit I. The presence of rare debris of marine molluscs and balls of *P. oceanica* helps to
45 304 characterize Unit II as part of a marine environment with high energy of deposition and where
46 305 occasional terrestrial input can be observed at roughly the midpoint of the Final Bronze Age. Unit II
47 306 can therefore be interpreted as a record of marine environments (intertidal to supratidal zone) with
48 307 two isolated fluvial inputs (Unit IIB); it shows similar features and a date close to that of Unit 1 in
49 308 Girolata 1 core.

54 309 - Unit III occurs between 1.50 and 0.40 m in depth. Age of deposition is well constrained and can
55 310 be dated from ca. 650 cal. BCE to 1650 cal. CE, based on the dating of three samples of rich organic
56 311 sediment (Table 2; Figure 6). It is composed of rich organic black clays (mean grain-size is around 5 to
57 312 10 μm) with generally high organic matter content, comprised between 10 and 32% and decreasing
58 313 towards the top of the unit. The highest values are recorded in the lowermost part of the unit with
59 314 peaks situated above 25%. Unit III does not attest the presence of marine molluscs, but plant remains

1
2
3 15 and large pieces of wood are identified. Pollen content is high and well preserved grains were identified
4 316 for reconstructing the past vegetation from the 7th century BCE to the 17th century CE (see section
5 317 5.2.2.). Unit III shows similar sedimentological features to Unit 3 in Girolata 1 core.

6
7 318 - Unit IV is found in the uppermost section of the core, from a depth of 0.40 m to the surface. It
8 319 consists of modern soils with the presence of light orange to brown silts.

9 320

10 321 4.1.3. Fangu core

11 322 The Fangu core is 4.20 m long and was drilled in the Fangu River estuary (Figs. 3A and 3B), which is
12 323 disconnected from the sea during summer. Three main sedimentary units have been identified (Fig. 7)
13 324 and no molluscs were identified along the sequence:

14 325 - Unit a is found from 4.20 and 3.50 m depth. It shows a transition from deeper layers of coarse
15 326 material, mainly composed of very coarse sands and angular gravels, to higher homogeneous marine
16 327 grey sands containing typical marine plant debris of *Posidonia oceanica* (top of the unit). A radiocarbon
17 328 dating was performed at 4.12 m deep and gave an age of 3945-3653 cal. BCE (Table 2), while the
18 329 uppermost part of the unit was dated to approximately 3 500 cal. BCE according to the depth/age
19 330 modelling (Figure 7).

20 331 - Unit b is situated from 3.50 to 3.15 m depth. It consists of coarse material with low organic
21 332 matter content (less than 5% on average), which increases towards the top. Sands and sharp gravels
22 333 of rhyolite suggest a continental input since this rock forms half of the geological formations of the
23 334 Fangu River. Age of deposition for Unit b is comprised between 3500 and 3100 cal. BCE (Figure 7).

24 335 - Unit c is located from a depth of 3.15 m to the surface and is relatively homogeneous (except
25 336 for the sandy/gravelly layer identified between 1.15 and 0.85 m in depth), with organic clayey sand
26 337 and peat layers. As a consequence, Unit c was studied for pollen identification (see below) which helps
27 338 to characterize the environment of deposition. Radiocarbon dating performed in the lowermost part
28 339 of Unit c (transition with Unit b) reveals an age of 3092-2907 cal. BCE (Table 2), which means that Unit
29 340 c has been deposited over the last five millennia. Organic matter content shows the higher values (>
30 341 10%) situated in the lowermost part of the unit: radiocarbon dating of these peaks reveals ages ranging
31 342 from 3092-2907 to 2925-2692 cal. BCE. Between 1.15 and 0.85m, a layer of coarse material can be
32 343 identified (Unit c1) which decreases gradually in terms of granulometry towards the top: the
33 344 lowermost part of this layer (1.15-1 m) is composed of rounded gravels and small pebbles embedded
34 345 within a clayey matrix, while the uppermost part (1-0.85 m) is characterized by coarse grey sands and
35 346 intercalated beds of small gravels. The age of Unit c1 cannot be directly obtained with ¹⁴C dating: the
36 347 depth/age model provides an estimated age from the 4th century BCE to the 4th century CE., roughly
37 348 corresponding to Roman times. In the upper part of the core (0.85 m deep to the surface), and
38 349 corresponding to the return to the homogeneous grey clays of Unit c, numerous micro- and macro-
39 350 charcoals are identified between 0.50 and 0.35 m, indicating a sustained fire activity: radiocarbon
40 351 dating performed at 0.48 m deep reveals an age of 1179-1277 cal. CE, corresponding to the Pisan
41 352 occupation of the island. It is likely that this rich charcoal content layer dates to the first half of the
42 353 second millennium CE.

43 354

44 355 4.2. Pollen results

45 356

46 357 4.2.1. The Girolata pollen record

47 358 Two main pollen zones and two sub-zones were defined using CONISS (Grimm, 1987; Fig. 8):

48 359 - Sub-zone A1 (417-125 cm; 1845-406 cal. BCE) shows moderate values of AP (ca.50%), predominated
49 360 by *Quercus ilex* and *Pinus*. In contrast, low values of *Quercus* deciduous, occurrences of *Fagus*, low
50 361 values of *Alnus* and *Olea* are reported. High values of *Erica* (up to 40%), showing a decreasing trend,

high values of *Vitis* to the end of this sub-zone. A peak of Poaceae and occurrences of Cerealia-t at 1.40 m (625cal. BCE). Low values of Cyperaceae and Amaranthaceae (Fig. 8). Among the NPP, a high abundance of Foraminifera remains at 4.12-2.98m and an increase in monolete spores, *Spirogyra*, *Glomus*, *Coniochaeta* cf. *Ligniaria* and occurrences of coprophilous fungi (*Sporormiella*, *Sordaria*-t, *Cercophora*-t) at 125-140cm (Fig. 8).

- Sub-zone A2 (120-90 cm; 290 cal.BCE-482 cal. CE) reveals a decreasing trend in AP where *Quercus ilex* remains the predominant tree. At the same time, we observe a decrease in *Pinus*, an increase in *Quercus* deciduous (Fig. 8) and an increase in riparian trees, mainly *Alnus*; high values of *Olea* are also reported. Peaks of Poaceae and Cerealia-t are identified at the beginning and at the end of the sub-zone, with an increasing trend in Asteraceae, Apiaceae, Cyperaceae and Amaranthaceae at the end of the sub-zone. Among the NPP, we note high values in monolete spores, a continuous curve of *Spirogyra*, a decrease in *Glomus* and the lack of coprophilous and lignicolous/carbonicolous fungi (Fig. 8).

- Zone B (80-50cm; 839-1461 cal. CE): there is a sharp decrease in AP (ca. 20%), *Quercus ilex* and *Olea*, and very low values of *Quercus* deciduous and *Alnus*. At the same time, a decreasing trend in *Erica* is reported with an expansion of Cistaceae along with high values of Poaceae and occurrences of Cerealia-t. High values in Asteraceae, Apiaceae, Cyperaceae and Amaranthaceae (Fig. 8). Among the NPP, high values in monolete spores, a decrease in *Spirogyra*, an expansion of *Zygnema*-t, *Rivularia* and *Pseudoschizaea*, occurrences of lignicolous-carbonicolous fungi (*Coniochaeta*, *Kretzschmaria*, HdV-6, *Chaetomium*, UAB-4, 9, 11, 38) and coprophilous fungi (*Sordaria*-t, *Sporormiella*). (Fig. 8).

4.2.2. The Fangu pollen record

Two main pollen zones and four sub-zones were defined using CONISS (Grimm, 1987; Fig. 9):

- Sub-zone A1 (200-190 cm; 2216-2082cal.BCE): high values of arboreal pollen (AP), predominated by *Pinus*, evergreen *Quercus* and riparian trees (*Alnus* spp., *Fraxinus*, *Salix*). This zone also shows low values of *Erica* and a remarkable peak of Cistaceae (Fig. 9).

- Sub-zone A2 (182-115 cm; 1962-507cal.BCE): we observe a slight regression in AP and *Pinus* and an expansion of *Erica*. High values of *Quercus ilex* and a slight decline in *Alnus* spp. are reported together with an increase in herb values (Poaceae, Asteraceae tubuliflorae, *Aster*-t) and a slight expansion in ferns (monolete spores, *Pteridium*, *Osmunda*-t and other trilete spores) (Fig. 9).

- Sub-zone B1 (83-66 cm; 316-740 cal. CE), a sharp decrease in *Pinus* values and later recovery (ca. 1500-1300 cal. BP) and opposite dynamics in *Erica*, expanding at *Pinus* regression.

- Sub-zone B2 (60-23 cm; 883-1632 cal. CE): minimum values of AP and *Pinus*, and a slight expansion of *Erica*. The expansion of NAP is predominated by Mediterranean shrubs (Cistaceae, *Helianthemum*-t, *Ephedra*, Lamiaceae) and grasses (Poaceae, Asteraceae, *Plantago*, *Artemisia*, Apiaceae). Occurrences of Cerealia-t at 28 and 34 cm (1435-1545 cal. CE). Occurrences of Amaranthaceae and Chenopodioidae and high values of Cyperaceae. Maximum values in monolete spores, *Polypodium*, *Isoetes*, *Pteridium* and *Osmunda*-t. Occurrences of *Pseudoschizaea* and type UAB-47 and maximum values of type HdV-36C.

401

402

403

404

405

5. Discussion

406

407

5.1. Palaeogeographic reconstruction of the coastal environments

408

09
410 5.1.1. Shoreline reconstruction of the Girolata Gulf for the Late Holocene (Middle Bronze Age-Medieval
411 Period/2200 cal. BCE-1800 cal. CE)

412
413 *Mid- to Final Bronze Age (1800-800 BCE)* - Based on the sedimentological analyses and the mollusc and
414 pollen identifications derived from Girolata cores 1 and 2, results indicate that the present day coastal
415 plain remained under shallow marine conditions during the Middle Bronze Age (from ca. 1800 to
416 1400/1350 cal. BCE; Fig. 10A). Indeed, a shallow and protected bay with a sandy-clayey bottom with
417 *Posidonia oceanica* seagrass was present. Our results confirm the previous chronostratigraphic results
418 obtained for the easternmost part of the area (Huser et al., 2017). During the whole period, for the
419 westernmost part of the present day coastal plain, the shoreline position was located approximately
420 150-175 m inland, while in the eastern part the coast was situated only 50 to 100 m further north, thus
421 creating a deeper marine incursion to the west.

422 Following this, during the Late Bronze Age (1400-1250 cal. BCE), only the westernmost part of the study
423 area was briefly occupied by a brackish lagoon (Fig. 10B), probably for less than a century in duration
424 while landscape configuration in the easternmost part remains uncertain due to the paucity of
425 chronostratigraphic data.

426 The Final Bronze Age (1200-800 cal. BCE) is characterised by generally higher energy of deposition than
427 was previously observed during the Mid- to Late Bronze Age. The influence of the local streams on the
428 coastal sedimentation is obvious and is confirmed by the presence of layers consisting of a mixture of
429 angular pebbles and gravels of both monzogranite and dacites with *Posidonia oceanica* remains. Of
430 note is the observation of a terrestrial input in the lower Novalla Stream valley only (Fig. 10C) at the
431 onset of the Final Bronze Age. However, this detrital input is not homogeneous and two distinct phases
432 of deposition composed of angular gravels of monzogranite embedded within an orange sandy matrix
433 (rich in quartz) are observed, separated by a brief phase of marine sedimentation dating to the 1119-
434 769 cal. BCE (median probability: 930 cal. BCE; Figure 6). The first phase of detritism, dated from ca.
435 1250-1150 BCE, can be related to a local phase of erosion that affected the monzogranitic bedrock,
436 situated primarily in the lowermost part of the Novalla catchment basin and in particular, on the
437 western hills where the small village of Girolata is located today. Similar high continental input, dated
438 to ca. 1200-1100 BCE, has been reported for the western coast of Corsica only, at the Canniccia pond
439 situated in SW Corsica (Ghilardi et al., 2017b; Vella et al., 2019) and at Crovani for the period 1250-
440 1150 BCE (Ghilardi, 2020; Di Rita et al., 2022a). Regional studies conducted around the Gulf of Lion in
441 the western Mediterranean also evidenced a phase of strong alluviation centred around 1200-1000
442 BCE, as is also the case in the Pyrenees (Galop et al., 2007) and in the lower Rhone River catchment
443 (Berger et al., 2007). The existence of the so-called 3.2 kyr cal. BP Rapid Climate Change (RCC) event is
444 suggested in the western Mediterranean with particular arid climate conditions (Mayewski et al., 2004;
445 Magny, 2004; Magny et al., 2007; Fletcher et al., 2013). The origins of this brief period of heavy run off
446 on the western coast of Corsica remain undetermined, but this area of the Mediterranean clearly
447 experienced episodes of intense precipitations during a phase of prolonged aridity, in particular at the
448 onset of the Final Bronze Age, ca. 1200-1100 cal. BCE.

449 Following a short return to marine conditions dated ca. 1000-900 BCE, at ca. 900-800 BCE, the Novalla
450 stream underwent a second brief alluvial crisis, mainly affecting the granitic bedrock, as is revealed by
451 the presence of an oxidized sandy layer. To the east, a large terrestrial input of the Girolata River is
452 also attested, flowing into the shallow marine bay and triggering a mechanism of southward shoreline
453 migration. Identification of this last phase of high continental detritism is based on the deposition of

1
2
3 54 sharp pebbles of rhyodacites and dacites that compose the upper reaches of the Girolata catchment.
4 455 However, the exact dating of this detrital input remains unknown, even if its early phase of deposition
5 456 can be dated approximately to the end of the Final Bronze Age/Early Iron Age, as suggested by the
6 457 chronostratigraphy of the Girolata 1 core (Fig. 5). Following this and as a direct consequence, a lowland
7 458 composed of coarse material deposited at the transition between the Final Bronze Age and the Early
8 459 Iron Age formed, situated inland of a large coastal barrier system that primarily formed to the east and
9 460 that advanced southwards. For the period 900-800 BCE, a mechanism of delta progradation based on
10 461 a migrating coastal barrier system has also been reported for the same period for the Sagone River
11 462 (Ghilardi et al., 2017a), situated approximately 30 km southwards. This morphological evolution of
12 463 river mouths has been also observed along the coast of Tuscany for the Ombrone River (Pranzini, 2001;
13 464 Bellotti et al., 2004; Biserni et van Geel, 2005) and in the Latium region for the Tiber River (Giraudi et
14 465 al., 2009; Giraudi, 2011). Possible direct consequences of the 2.8 kyr cal. BP Bond event 2 (Iron
15 466 Age/Homeric minimum; Bond et al., 1997), a period recognized for its sustained hydrological activity in
16 467 the Western Mediterranean (Basetti et al., 2016), have been put forward to explain such deltaic
17 468 advances. For the moment, there is no palaeoclimate reconstruction established for Corsica, so this
18 469 question remains challenging, in particular along the western coast of the island.
19
20
21
22
23
24

25 471 *Iron Age, Roman and Medieval periods (800 BCE- 1800 CE)* - During the Iron Age and Roman times (Fig.
26 472 10D), shoreline migration decelerated and enabled the formation of a large coastal barrier that
27 473 extended along the entire paleo Bay of Girolata. To the west, a large coastal swampland developed
28 474 with no significant detrital input from the Novalla Stream, from the Early Iron Age until modern times.
29 475 The pollen record points to a freshwater environment, which was testified from 700 cal. BCE by high
30 476 values of freshwater algae and riparian trees such as *Salix* and *Tamarix*. Then, a change towards a sub-
31 477 aerial brackish marshland dominated by Cyperaceae and Amaranthaceae, with remarkable amounts
32 478 of Apiaceae and ferns began around 550 cal. CE. This local environment persisted until the reclamation
33 479 works of the plain in the 20th century CE (Fig. 10E). The regression of arboreal taxa and the high
34 480 dominance of Asteraceae at 0.70-0.50 m at Girolata suggests soil formation (transition to a terrestrial
35 481 environment) edaphisation for the last millennium according to the chronostratigraphy (Figure 6). In
36 482 conclusion, the Roman period coincides with a more humid phase attested by the existence of a
37 483 freshwater wetland, suggesting that wetter conditions and the availability of freshwater favoured the
38 484 establishment of human populations in coastal areas of western Corsica during the Iron Age and the
39 485 Roman period.
40
41
42
43
44
45

46 487 *5.1.2. The Fangu Estuary: evolution over the last six millennia*

47 488 The sedimentary sequence collected in the Fangu Estuary reveals the presence of two main
48 489 environments with contrasted energy of deposition. From ca. 4200 to 3500 cal. BCE, a marine
49 490 environment prevailed in the western part of the present-day estuary (coring site). The presence of
50 491 balls of *Posidonia oceanica* embedded within coarse sands and gravels indicates a high energy of
51 492 deposition, probably related to an open marine bay. In the Mediterranean, the Mid-Holocene
52 493 corresponds to a period of maximum sea incursion inland (Vacchi et al., 2016; 2018). Elsewhere in
53 494 Corsica, this Mid-Holocene maximum marine incursion has been dated to 4000-3500 cal. BCE on the
54 495 eastern coast, in the Aleria-Del Sale area (Currás et al., 2017) and on the North-West coast at Saint-
55 496 Florent (Revelles et al., 2019). At both the Aleria and Saint Florent sites, the marine incursion was
56 497 followed by a deceleration in sea-level rise that favoured the formation of coastal wetlands, mainly
57
58
59
60

1
2
3 98 lagoonal environments. Similar observations have also been reported in the Eastern Mediterranean
4 499 with the onset of delta formations dated around 3500 cal. BCE (Brückner et al., 2005).
5 500 In the Fangu Estuary, the marine environment was followed by a phase of detrital input, probably
6 501 linked to a deltaic advance of the Fangu River from ca. 3500 to 3100 cal. BCE. Isolation of brackish
7 502 water behind a coastal spit favoured the formation of coastal wetlands shortly after that date.
8
9 503 From ca. 3000 BCE until the present day, generally calm environments of deposition related to the
10 504 formation of coastal wetlands have been recorded. However, a brief interruption in wetland
11 505 deposition occurred from ca. 400 cal. BCE to 400 cal. CE marked by a fluvial input that persisted roughly
12 506 throughout Roman times. The literature contains little evidence for such detrital input from Corsican
13 507 rivers during Roman times, however an anthropogenic destabilization of the soils in the upper reaches
14 508 of the Fangu River cannot be ruled out as a possible influence of this process. Climate conditions during
15 509 the Roman period in the Mediterranean are recognised as being warm and wet, which possibly induced
16 510 reinforced runoff in a context of diminished forest cover. As a result, the Fangu catchment may have
17 511 experienced reinforced alluviation. Since the end of Roman times, landscape configuration has
18 512 remained stable with the presence of coastal wetlands with salt intrusions. Our pollen record suggests
19 513 that the Fangu lagoon may have been surrounded by riparian forests dominated by *Alnus*, *Fraxinus*,
20 514 and *Salix* species, with prevailing freshwater conditions. Companion hygrophilous species of these
21 515 riparian trees also seen to increase during this time interval are Cyperaceae and ferns (e.g. *Pteridium*,
22 516 *Osmunda-t*, and other ferns with monolete spores (Figure 9). During the Middle Ages (750 cal. CE
23 517 onwards), the development of Cyperaceae (Figure 9) reflects the expansion of shore environments
24 518 leading to a regression of the lagoon and the expansion of sedges. Finally, the decline of sedge
25 519 vegetation and the development of fern-dominated environments suggest drier conditions at local
26 520 scale.
27 521 In general, prevailing freshwater conditions throughout the Late Holocene are also testified by the
28 522 continuous record of freshwater algae, accompanied by low values of Amaranthaceae.
29 523

30 524 5.2. Vegetation history of the UNESCO protected site (Fangu and Girolata coastal plains) and the 31 525 influence of rapid climate changes during the Late Holocene

32 526 The palynological study of cores Girolata 2 and Fangu enables the reconstruction of landscape for NW
33 527 Corsica over the last 4200 years, from the Early Bronze Age to the Middle Ages. This helps to complete
34 528 previous research conducted in the 1990s in the Fangu Estuary (Reille, 1992a) and in the 2020s in the
35 529 Crovani pond (Di Rita et al., 2022a), respectively.
36 530

37 531 *Bronze Age (4150-2750 cal. BP/2200-800 BCE)* - For the Porto Gulf UNESCO site, the vegetation has
38 532 always been predominated by Mediterranean maquis, configuring an open landscape with *Erica* and
39 533 Cistaceae, especially in Fangu, where *Erica* reaches 40-50% values (Figure 9). Pine and sclerophyllous
40 534 forests played a secondary role in Girolata 2, while *Pinus* shows an important role in the area of Fangu,
41 535 especially during the first half of the sequence (4200-2400 cal. BP/2250-450 cal. BCE). Mesic forests
42 536 (*Quercus* deciduous, *Betula*, *Corylus*, *Tilia*, *Carpinus*) had a limited role in the landscape during the Late
43 537 Holocene in this area, suggesting that climate conditions were more favourable to sclerophyllous
44 538 vegetation in the lowlands. Of note is the limited presence of *Alnus* spp. riparian forests in this area
45 539 compared with other Corsican areas, such as Saint Florent in the north (Revelles et al., 2019), Del Sale
46 540 and Palo on the eastern coast (Currás et al., 2017; Revelles et al., 2019) and Sagone on the western
47 541 coast (Ghilardi et al., 2017a). This may be due to the predominance of *Pinus pinaster* and *Pinus laricio*,
48 542 accompanied by a maquis understory in granitic substrates at lower altitudes, as also occurs today in
49 543 this area of Corsica. This would explain higher values in *Pinus* than *Quercus ilex* in Fangu, and the

1
2
3 44 limited presence of *Alnus* in both records. In this sense, during the period ca. 4200-2750 cal. BP (2250-
4 545 800 cal. BCE/Bronze Age), pine forests played a significant role in the landscape in Fangu (Fig. 9),
5 546 accompanied by *Erica*-dominated maquis.

6 547 Interestingly, from 4200 to 3900 cal. BP (2250-1950 cal. BCE) *Pinus* forest and *Erica* maquis declined,
7 548 favouring the development of a Cistaceae-dominated shrubland. This forest dynamic may have been
8 549 triggered either by land clearing practices of anthropogenic origin or by a climate change linked to the
9 550 4.2 kyr BP event, corresponding to the Bond event 3 (Bond et al., 1997; Figure 11), but the evidence is
10 551 too scanty to be attributable to one cause or the other. As there are no known Early Bronze Age sites
11 552 in this area of Corsica, an anthropogenic origin for this sudden change in vegetation cover is therefore
12 553 highly hypothetical. As for the 4.2 kyr BP event, this climate change does not appear to be associated
13 554 to any general deforestation patterns in Corsica (Di Rita et al., 2022a, b). Conversely, several pollen
14 555 sites show forest development (refs). We can therefore only speculate that an arid climate event, if
15 556 one occurred, had only a limited impact on intermittent coastal ecosystems.
16 557

17 558 *Roman times to the end of the Genoese period (2450-150 cal. BP/500 BCE-1800 CE)* - Mixed forests of
18 559 *Pinus* and *Quercus ilex*, accompanied by maquis of *Erica* were the predominant component of the
19 560 landscape until the change of era, when forest decline led to the expansion of maquis, predominated
20 561 by *Erica* and with an increasing role of Cistaceae (Figs. 8 and 9). Until Roman times, human impact was
21 562 limited in the evolution of forest cover in terms of short-term deforestation episodes and rapid
22 563 recovery, consistent with previous studies in the area (Di Rita et al., 2022a). Only at Girolata can we
23 564 report two brief episodes of forest decline dated at ca. 450 and 200 cal. BCE, mainly affecting the *Q.*
24 565 *ilex* cover.

25 566 During Roman times (250 cal. BCE-400 cal. CE), the high values of *Quercus* suggest an expansion of oak
26 567 forests in NW Corsica, possibly triggered by an increase in summer rainfall during the Roman Warm
27 568 Period (RWP). These climate conditions also led to the development of freshwater swamps in the
28 569 Girolata coastal plain (Figures 6 and 10). Subsequently, and following Roman Empire, deforestation
29 570 processes and major changes in vegetation composition occurred. Indeed, from 500 CE onwards,
30 571 regression of *Quercus* spp. values is evident in Girolata 2 and Fangu records, as is the decline of oak
31 572 woods that began at the change of era in the area of Crovani and which is consolidated during this
32 573 period. The Early Medieval cooling episode (500-900 cal. CE), also known as the Dark Ages or Migration
33 574 Period Cooling (Ljungqvist, 2010) may be linked with this decline in oak woodland. This episode is
34 575 clearly evidenced by minimum $\delta^{18}O$ in GISP2 (Figure 13) and coincides with the 1.4 kyr cal. BP Bond
35 576 event 1 (ca. 550 cal. CE; Bond et al., 1997), with RCC 1 (1.2-1.0 kyr cal. BP/750-950 cal. CE) defined in
36 577 Mayewski et al. (2004). This period marked the transition from Late Antiquity to the Early Middle Ages
37 578 when a strong human migration occurred in Europe between 300-700 cal. CE (Wanner et al., 2011).
38 579 Finally, the strong human impact in the four pollen records during the first half of the second
39 580 millennium CE (1000-1500 CE) leading to forest decline prevented from contrasting *Quercus* spp.
40 581 curves with climate conditions from this phase onwards. Consequently, evidence from the NPPs record
41 582 shows high concentrations of carbonicolous-lignicolous fungal spores in these chronologies in the
42 583 Girolata pollen diagram (Figure 8) and numerous charcoals for Fangu core. These fires, associated to
43 584 peaks in anthropogenic indicators, are interpreted as human-induced in other records (Lestienne et
44 585 al., 2020; di Rita et al., 2022a), and explain the important role of fire in vegetation dynamics in the
45 586 Mediterranean.
46 587

47 588 5.3. Human impact on coastal landscape evolution of North-Western Corsica

48 589
49 590 Figure 11 summarizes the recent pollen results acquired for four sites from the north western area of
50 591 Corsica: published data from the Saint Florent and Crovani sites (Revelles et al., 2019; Di Rita et al.,

92 2022a) are combined with results obtained for the present study from the Fangu and Girolata sites.
 593 Arboreal pollens are associated with anthropogenic markers in order to evaluate the timing of human
 594 impact on the vegetation composition with a possible identification of climate control during Bond
 595 events.

596

597 5.3.1. For the UNESCO site (Fangu and Girolata coastal plains)

598 *Protohistory (Bronze Age: ca. 2200-800 cal. BCE)* – Evidence of human impact during the Bronze
 599 Age is scarce and is restricted to the southern part of the UNESCO site only, in the region of Girolata
 600 (Fig. 11). This site evidences agriculture during the Middle Bronze Age (1600-1350 cal. BCE, Phase 2;
 601 Figure 11), a period when the sites of human occupation (*I Casteddi/Castles*) were located primarily on
 602 the top of hill mounds or rocky outcrops (Pêche-Quilichini, 2015a and 2015b). Until now, no
 603 archaeological surveys confirming the presence of such a Middle Bronze Age site have been conducted
 604 in the UNESCO area, but in the near future archaeological prospections could include this cultural
 605 period and not only Medieval times. Cereal cultivation, though scarce, is attested during the Middle
 606 Bronze Age in the surroundings of the present day Girolata coastal plain. No indication of land-use is
 607 available for the Final Bronze Age (1200-800 cal. BCE) due to poor pollen preservation in the Girolata
 608 sequence, and to a lack of anthropogenic markers in the Fangu estuary area.

609

610 *Early Iron Age - Roman times (800 cal. BCE-500 cal. CE)* – Pollen results of both coastal sites clearly
 611 indicate that human activities have affected the vegetation composition for the previous 2000 years,
 612 and locally for the last 2500 years, with a significant and continuous impact on the forest cover starting
 613 from ca. 1650 cal. BP (300 cal. CE) and affecting both areas simultaneously. In addition, the Girolata 2
 614 core shows evidence of agriculture during the whole Roman period (Phase 3; Figure 11), starting from
 615 ca. 450 cal. BCE to the 6th century CE with two intermittent phases of forest retreat dated ca. 450 and
 616 200 cal. BCE. Two main agricultural phases can be distinguished (Figures 8 and 11): the first one dates
 617 from the 5th century BCE to the onset of the common era and combines both cereal cultivation and
 618 husbandry, as indicated by the presence of coprophilous fungi. The strong presence of *Vitis* during a
 619 short period of time over the Roman Republic (from ca. 500 to 350 cal. BCE; Figure 8) can be reasonably
 620 associated with grapevine cultivation on the hills surrounding the Girolata coastal wetland. The second
 621 phase ranges from the onset of the common era to the 6th century CE (Roman Empire) and is marked
 622 by a near- exclusive agricultural activity based on olive tree cultivation (*Olea* in Figure 8). At the onset
 623 of the common era, the sudden change in terms of land use around the Girolata coastal plain can be
 624 related to the major political changes that occurred in Rome during the transition from the Roman
 625 Republic to the start of the Roman Empire. The Roman Empire established a distinct specialisation
 626 concerning the type of agriculture undertaken in each province, a practice which can be inferred for
 627 Corsica, as well as in Northern Africa (Leveau, 1990). A clear and continuous agricultural activity is
 628 evidenced for the first time in Corsica in the Girolata sequence and in the vicinity of archaeological
 629 remains dating from throughout the Roman period (almost one millennium in duration). This confirms
 630 the geostrategic importance of both Girolata Bay and its coastal plain under the Roman domination of
 631 the Mediterranean. The Fangu site shows no clear human impact prior to the onset of the common
 632 era. The regression of pine forests and the progressive expansion of *Erica* maquis from 1600 cal. BP
 633 onwards (Figure 9) is best interpreted in the light of increasing human impact during Roman times,
 634 thus confirming Reille's vegetation pollen-based reconstruction (Reille, 1992a). However, the low
 635 resolution of the sequence pertaining to that period as well as the deposition of sands at 1.15-0.85m
 636 for the Fangu core make it difficult to study the socio-environmental dynamics during the Roman
 637 period.

638

1
2
3 639 *Late Antiquity, Medieval times, Pisan, and Genoese administrations of the island (500 cal. CE-Late*
4 640 *18th century CE)* - At Fangu, Late Antiquity and the Medieval period correspond to phases of strong
5 641 human impact on forest ecosystems of the island. The lowest values of arboreal pollen date to ca. 1150
6 642 cal. CE and 1400 cal. CE, respectively (Figure 9), and reflect intense human activities during both the
7 643 Pisan and Genoese administrations of the island. Forest decline during the Middle Ages was also
8 644 reported at Crovani (Di Rita et al., 2022a; Fig. 1), situated only 6 km to the north, and at Saint Florent
9 645 (Revelles et al., 2019). Reille's investigations at Fangu (Reille, 1992a) suggested that *Q. ilex* in the high
10 646 Fangu valley probably replaced a burnt *P. laricio* forest around 1500 cal. BP. This anthropogenic
11 647 disturbance mainly affected pine forests and *Erica* maquis, indicating deforestation processes both in
12 648 the lowlands and uplands of the region. The presence of Cistaceae over the last 1500 years at Girolata
13 649 (Figure 8) and over the last 1000 years at the Fangu site (Figure 9), combined with a high abundance
14 650 of charcoal particles as observed and described during sedimentological analyses (no quantitative
15 651 charcoal data are available at the moment) from ca. 1000 to 1500 cal. CE at the Fangu site reinforces
16 652 the regular occurrence of fires within and in the vicinity of the UNESCO site. At Fangu, evidence of
17 653 cereal cultivation is recorded solely during the Genoese administration of the island (Phase 4; Figure
18 654 11), coeval with the building of the defensive towers during the 16th century CE in the vicinity of the
19 655 Fangu estuary (Figs. 3A and 3B). Human disturbance probably explains the expansion of Mediterranean
20 656 shrublands (*Erica*, Cistaceae, *Helianthemum-t*, *Ephedra*) and grasslands and ruderals (Poaceae,
21 657 Asteraceae, *Plantago*; Fig. 9). The fact that no cereal cultivation is observed in the vicinity of the Fangu
22 658 estuary prior the Genoese period reinforces the idea that this area was not of strategic interest for
23 659 agricultural purposes, unlike the Girolata Plain which was certainly a major site in Corsica throughout
24 660 Roman times.

25 661
26 662 *5.3.2. In NW Corsica: Nebbiu, Balagne and Filosorma areas*

27 663 *Prehistory (Late to Final Neolithic times, 3900-2200 cal. BCE)* - Figure 11 shows evidence for agriculture
28 664 and husbandry that points to an episode of human impact at the onset of the Late Neolithic (ca. 3900
29 665 cal. BCE) in both Crovani and Saint Florent, with a limited impact on the forest cover (Human Impact
30 666 (HI) episode 1; Figure 11). Following this, the Final Neolithic (2800-2200 cal. BCE) was a period of
31 667 important agricultural development in NW Corsica, notably at Crovani (Di Rita et al., 2022a) and at
32 668 Saint Florent (Revelles et al., 2019). Both of these sites record cereal cultivation and husbandry along
33 669 the coastal zone within an environmental context of swampland, with a generally moderate impact of
34 670 human activity on the forest cover (AP decline; Figure 11). It is noteworthy that a moderate forest
35 671 decline is simultaneously observed at the onset of the Final Neolithic at Crovani and at Saint-Florent
36 672 (ca. 2800-2600 cal. BCE, Phase 1; Figure 11), corresponding to a phase of agricultural development
37 673 along the shoreline (Phase 1; Figure 11).

38 674
39 675 *Protohistory (Bronze Age, 2200-800 cal. BCE)* - Following the Neolithic period, the Early Bronze Age
40 676 shows little evidence of anthropogenic activities for NW Corsica, and this period is also largely marked
41 677 by a paucity of sites of human occupation. In contrast, the period covering the Middle to Final Bronze
42 678 Age (Phase 2, Figure 11) reveals a return to agricultural practices in the coastal areas at Girolata,
43 679 Crovani and Saint Florent. A second phase of forest decline of moderate importance, consisting of
44 680 short-term forest decline episodes followed by a rapid recovery, is observed during the Middle Bronze
45 681 Age (Phase 2; Figure 12) which is a cultural period marked by the development of fortified castles (*/*
46 682 *Casteddi*; Pêche-Quilichini, 2015b) on inland hilltops overhanging alluvial valleys (Ghilardi et al.,
47 683 2017b). This type of site was clearly linked to isolated forest clearings and agricultural development,
48 684 with grain storage inside the structures behind defensive walls. However, only low levels of cereal
49 685 cultivation and scarce occurrences of husbandry are evidenced at Girolata (Phase 2, Figure 11), mainly

1
2
3 686 during the Middle Bronze Age. It seems that Fangu estuary was less favoured for agriculture at that
4 687 time. The presence of the Fangu River associated with a flooding exposition of the area provides a
5 688 reasonable explanation for such low agricultural activity in the lowlands
6 689

7 689
8 690 *Early Iron Age - Roman times (800 cal. BCE-500 cal. CE)* – For the later Iron Age to Roman period, a
9 691 major regional change with clear human impacts on the vegetation composition can be observed.
10 692 During the Iron Age, evidence of cereal agriculture at Girolata and at Crovani, and probable *Vitis*
11 693 cultivation around Girolata, are associated with moderate impact on forest cover (HI episode 2; Figure
12 694 11). Agricultural development can thus be linked to a third phase of forest decline starting around the
13 695 onset of the 5th century BCE at Girolata, Fangu and Crovani (Phase 3; Fig. 11), while forest decline in the
14 696 area of Saint Florent appears approximately one millennium later (Figure 12). Similar observations of
15 697 forest decline have also been reported for SW Corsica (Vella et al., 2019) and slightly earlier (2500
16 698 years BP), on the Eastern coast (Currás et al., 2017), thus confirming Reille's conclusions concerning
17 699 dating of the first important anthropogenic impacts on Corsican vegetation composition since the
20 700 onset of Roman times (Reille, 1992a). Different dynamics are observed in Saint Florent and Girolata 2:
21 701 human impact affected mainly *Alnus* spp. forests and to a lesser extent secondary pine forests (Revelles
22 702 et al., 2019) in Saint Florent, but predominantly pine forests in Girolata (Figure 8). The Crovani record
23 703 provides evidence of probable cultivation of olives during the Roman period (Di Rita et al., 2022a), a
24 704 suggestion that may also be valid in the case of Girolata, where a peak of *Olea* led to a peak in the OVJC
25 705 Index (Phase 3; Figure 11) during the Roman period. Anthropogenic activities during Roman times
26 706 (Roman Republican) did not significantly affect forest cover or vegetation composition in general,
27 707 whereas during the Roman Empire (at the onset of the common era) forest cover substantially
28 708 declined.
29 709

31 709
32 710 *Late Antiquity, Medieval times, Pisan and Genoese administrations of the island (500 cal. CE-Late*
33 711 *18th century CE)* - From the pre-Christian era until the end of the Genoese administration of the island,
34 712 human activities deeply impacted the pine forest (Phase 4; Figure 12). Reille (1992a) suggests that
35 713 frequent fires burnt the *Pinus laricio*, a finding supported by our record from Fangu which reveals a
36 714 large number of micro- and macro charcoals (not identified for the present study) in the 0.50-0.35 m
37 715 depth range, roughly corresponding to the first half of the second millennium CE. To explain this
38 716 decline, forest exploitation must also be examined through literary sources. Indeed, manuscripts
39 717 dating from the Genoese administration of the island reveal that Corsican forests were exploited for
40 718 their wood (see section 5.3.3. below). In addition, due to incursions of vandalism in the Corsican coastal
41 719 areas and lowlands, the inhabitants were forced to migrate away from the coast and in doing so, the
42 720 need for wood to build villages was substantial. The combination of forest exploitation and repeated
43 721 fires provoked a rapid and strong reduction in forest cover during a period of political instability
44 722 following Roman times.
45 723

46 723
47 724 At the scale of the large Western Mediterranean islands, our results are consistent with palynological
48 725 studies conducted on Minorca (Balearic Islands), where the Iron Age was a period of intense human
49 726 activity and where landscape transformation during Roman times is evident in numerous records, such
50 727 as at Algendar and Es Grau in Minorca (Yll et al., 1997; Burjachs et al., 2017). This is evidenced by the
51 728 regression of AP, the expansion of maquis and the occurrence of *Cerealia-t*; and Prat de Vila (Ibiza;
52 729 Burjachs et al., 2017), and also by the regression of pine forest, the expansion of maquis and
53 730 grasslands, and the occurrence of *Cerealia-t*. In addition, on the Iberian Peninsula during the Roman
54 731 period, large-scale deforestation resulted in open landscapes characterising lowland areas as a
55 732 consequence of the intensification of human activities such as cropping, grazing, mining or forestry.
56 733 Nevertheless, the decline of western Mediterranean forests, although initiated during the Roman

734 period, really began from the 10th century CE onwards (López-Sáez et al., 2015). Finally, the pollen
 735 record of the Tirso coastal plain in Western Sardinia points to a clear open vegetation rich in
 736 synanthropic herbs during the last millennium (Melis et al., 2017).

738 5.3.3. On the question of the exploitation of Corsican wood resources from Roman times onwards

739
 740 Whereas archaeology has revealed little evidence regarding the exploitation of the forests of Corsica
 741 during the historical period, the scrutiny of historical sources can provide precious information about
 742 the exploitation of wood on the island (Rotta and Cancellieri, 2001). Indeed, the vegetation
 743 reconstruction carried out in the UNESCO site for the present study has confirmed descriptions
 744 recorded by ancient writers in documents spanning the last 2500 years.

745 The first event (Figure 12) of wood exploitation dates back to Early Roman times. The oldest
 746 literary source to record this event can be found in descriptions made by Theophrastus (371-288 BCE),
 747 who mentions an expedition for the recovery of wood. An attempt to build a city specialized in the
 748 intermittent exploitation of the resource between 377 and 311 BCE was planned. Activities there
 749 undoubtedly concerned the Laricio pine, defined by Teophrastus as “the largest of all” (*Historia*
 750 *Plantarum*: V.8). This text reports the presence of many gulfs and shelters testifying to a high likelihood
 751 that the later Roman expeditions most certainly took place on the western coast. During a short period
 752 of time, the Romans deforested a large amount of wood in a "small area" a short distance from the
 753 coast. The estimated date of the expedition fits tightly with the palynological results obtained for the
 754 present study, which indicate significant human impact on forest cover, particularly in the area of
 755 Girolata where pine forests regressed around 400 BCE (Figures 8, 11 and 12). It appears that this
 756 exploitation was tied to the provisioning of materials for shipbuilding.

757 The second event also took place during the Roman Republic at around 200 BCE in the area of
 758 Girolata, but no known ancient documents mention forest exploitation at that date.

759 The third event took place around the 4th-5th centuries CE (Figure 12). Victor de Vita writes in
 760 about 486 CE (*History of the persecution of the Vandals*: V. 5) that a small number of Catholic bishops
 761 from Africa were deported to the island for the exploitation of the forest. Despite the low number of
 762 deportees mentioned, the pollen results agree with this historical fact and show the onset of a
 763 deforestation process in the Fangu-Girolata area which also impacted oak forests (Figures 8, 9 and 11).

764 The fourth attested event of forest opening (Figure 12) took place during the first Muslim
 765 invasions in the Mediterranean in around 717 CE when the Constantinople expedition was organized
 766 in the quest for raw materials necessary for the construction of their fleets (Lombard, 1959 and 1972).
 767 The search for sources of wood was persistent throughout the 9th and 10th centuries CE, and due to
 768 clashes between the naval powers of the Caliphate and the Byzantine Empire, resources dwindled and
 769 became the object of smuggling. As a direct consequence, Muslim invaders began to attack the coasts
 770 of Anatolia, Dalmatia, Sardinia and Corsica (Lombard, 1972) in their search for wood. Strong evidence
 771 of deforestation during this period is attested around Girolata, where the lowest AP values in the Late
 772 Holocene in NW Corsica can be seen where human impact led to the abrupt regression of oak
 773 woodlands and prevented the recovery of pine forests (Figure 8). In the case of Fangu, the decline of
 774 arboreal pollen from 700 CE onwards coincides with the Muslim invasions, during which the majority
 775 of wood exploitation focussed on pine forests (Figure 9). The Crovani area also experienced strong
 776 forest decline during this period (Di Rita et al., 2022a), suggesting that the Girolata-Fangu-Crovani area
 777 was regionally affected by forest clearance beginning in the 7th-8th centuries CE.

778 The fifth event can be observed during the Pisan and Genoese dominations of the island
 779 between the 11th and 16th centuries CE (Figure 12). Archaeological data attest to changes in population
 780 rhythms and settlement dynamics accompanied by a new colonization of spaces at the onset of the

1
2
3 781 2nd millennium CE (Mary, 2011, 2012, and 2020) when the demand for wooden constructions such as
4 782 scaffolding, planks, beams and frames became significant. The Pisan colonization of the island (1070-
5 783 1284 CE) required that certain areas be cleared to permit cultivation of the land: the forest cover
6 784 therefore underwent a strong decline. This is revealed by the pollen diagrams from both Girolata Plain
7 785 (Figure 8) and the Fangu estuary (Figure 9), with additional forest regression attested in Crovani and
8 786 Saint Florent in the same chronologies (Phase 4, Figure 11). During this period, strong evidence of
9 787 farming activities is documented in the area of Girolata, with high values of cereal pollen and
10 788 coprophilous fungi suggesting the practice of animal husbandry in the surrounding areas (Figures 8 and
11 789 11). At the beginning of the 16th century CE (1510 CE), the Republic of Genoa took full possession of
12 790 the island and the generalised exploitation of the island's forests began. This supports the fourth phase
13 791 of human impact and deforestation as defined by pollen analysis (Figures 11 and 12). The impact of
14 792 farming activities during this period is also attested in the Fangu area (Figure 9), suggesting
15 793 demographic growth or expansion of human communities in the territory. The Office of Saint Georges
16 794 of the Genoese Republic established the first project (Della Grossa et Montegiani, 2016), including the
17 795 western coast of Corsica which was the most popular region according to descriptions recorded by
18 796 Monsignor Giustiniani (Giustiniani, 1993), who also mentions that the wood from the mountain sector
19 797 surrounding Galeria was transported to the coast and that the inhabitants of Calvi traded it both
20 798 domestically and off-island. The full development of wood exploitation was set up in the 17th century
21 799 CE with the development of inland exploitation at Aitone or Guagno where the trees were older,
22 800 straighter, taller, and of a higher quality, according to the Dutch captain Cornelius de Witt who was
23 801 dispatched there by the Genoese in 1639 (Archivio di stato di Genova, 1639). This development
24 802 towards the exploitation of the island's interior woodlands is a clear example of landscape degradation
25 803 through the intensive exploitation of NW Corsican coastal forests which took place during the Middle
26 804 Ages and early Modern Age. Similarly, this shift toward inland resources may also explain the coastal
27 805 forest recovery attested in pollen diagrams for the area of Fangu and Crovani from 1600 CE onwards
28 806 (Figure 12).

807

808 6. Conclusions

809 The multidisciplinary dataset obtained for both the UNESCO site of Scandola-Galeria and the NW area
810 of the Corsican regional park helps to reconstruct past human-environment interactions over the last
811 six millennia for the first time. The main outcomes of the present work are summarized as follows:

- 812 1. The coastal plains of Girolata and Fangu formed at different times: formation of the Fangu
813 deltaic plain began around 3500 cal. BCE following the "classical" scenario observed for most
814 of the large Mediterranean deltas. The Girolata coastal plain is much younger and mainly
815 formed from the mid-second millennium BCE to the mid-first millennium BCE. The Girolata
816 plain formation shows similar features with nearby deltaic plains such as at Sagone, situated
817 ca. 25 km southwards (Figure 12) and the coastal plains of Tuscany (Ombrone and Magra
818 Rivers) and Latium (Tiber River).
- 819 2. The northern part of the UNESCO site (Fangu estuary) is scarcely affected by anthropogenic
820 activities until the mid-first millennium CE, while the southern part (Girolata coastal plain)
821 records human impacts on the vegetation composition beginning in approximately the Mid-
822 first millennium BCE, corresponding to the onset of the Roman Republic. Before any human
823 impact, forest vegetation composition was characterised by the predominance of a dense
824 maquis with predominance of *Erica* sp. in the coastal area, as was recorded by Maurice Reille,
825 and which has also recently been confirmed by the pollen-based vegetation reconstructions
826 for the nearby Crovani (Di Rita et al., 2022a) and Saint Florent (Revelles et al., 2019) areas.

- 1
2
3 827 3. The Girolata Plain and its surroundings was an important site of human occupation during
4 828 Roman times from the 5th century BCE until the 6th century CE, and benefitted from favourable
5 829 environmental conditions for the development of agriculture, with the presence of a
6 830 freshwater swamp throughout Roman times. It is clear that the sheltered bay of Girolata
7 831 served as a natural harbour for the importation of goods for approximately one millennium.
8 832 Evidence of land use in the environs of the Girolata Plain reveals the presence of agricultural
9 833 communities who first practiced cereal cultivation and viticulture alongside livestock breeding
10 834 during the first phase of Roman times (5th century BCE-1st century CE, Roman Republic), and
11 835 who then developed a dominant *Olea* cultivation which superseded cereal cultivation and
12 836 livestock breeding during the second phase (1st-6th centuries CE, Imperial Period). The Girolata
13 837 pollen sequence is one of the rare Corsican, and even western Mediterranean sequences, to
14 838 fully reconstruct human impacts (including land-use practices) on the vegetation composition
15 839 throughout Roman times. To the north, in the Fangu catchment, a period of reinforced alluvial
16 840 activity is observed throughout Roman times and may be explained by changes in land-use in
17 841 the uplands related to the Girolata inland forest exploitation. Further palynological
18 842 investigations will undoubtedly provide more accurate documentation of vegetation
19 843 composition in the northern area of the UNESCO site during Roman times.
- 20 844 4. The UNESCO site began to be affected by the strong impact of human activities from the mid-1st
21 845 millennium CE, with significant and widespread clearing of upland pine forests and lowland
22 846 maquis starting in Roman times. Potential upland forest clearance may have provoked
23 847 reinforced alluvial activity of the Fangu River during the Roman Warm Period (RWP),
24 848 characterized by regionally wet climate conditions. The substantial reductions of forest cover
25 849 were greatest during the Middle Ages, when pollen records indicate the lowest cover over the
26 850 past four millennia, and throughout the Pisan-Genoese administration of the island,
27 851 confirming regional observations made to the north and northeast in the Crovani and Saint
28 852 Florent areas, respectively. Wood resources were intensely exploited during the Pisan-
29 853 Genoese colonization of Corsica leading to minimum expansion of the woodland during the
30 854 Late Holocene.
- 31 855 5. Vegetation changes represented by the replacement of *Erica*-dominated maquis by Cistaceae-
32 856 dominated shrubland is recorded in the Fangu pollen record and may be linked either to
33 857 human activities or to local effects of the 4.2 kyr cal. BP climate event (Bond event 3).
- 34 858 6. Detrital input is recorded at ca. 3.2 kyr cal. BP and reveals a possible climate control on the
35 859 sediment dynamics of the local streams, related to the 3.2 kyr cal. BP RCC event. This event is
36 860 also evidenced for several coastal plains situated on the western coast of Corsica and around
37 861 the Gulf of Lion.
- 38 862 7. The 2.8 kyr cal. BP event (Bond event 2, Homeric Minimum) has been hypothesised as a driving
39 863 factor of a phase of major fluvial input recorded in the Girolata area, and is also probably linked
40 864 to a shoreline progradation pattern at regional scale.
41 865

866 Funding and acknowledgements

867 The studies at Girolata and Fangu were undertaken in 2020 and 2021, respectively, within the
868 framework of the PhD thesis of Jean-Baptiste Mary (University of Lyon II/Collectivité de Corse). This
869 article is a contribution to the PCR "Approche géoarchéologique des paysages de Corse à l'Holocène,
870 entre mer et intérieur des terres « Tra Mare à Monti »" programme (2018-2020), funded by the DRAC
871 Corsica (Ministry of Culture) and directed by Matthieu Ghilardi. The Regional Park of Corsica is
872 acknowledged for providing substantial field assistance during coring campaigns. The authors are
873 grateful to Jean-François Luciani for his precious help during summer 2020 fieldwork in Girolata.

874 Jordi Revelles is a member of the GAPS (2017 SGR 836) research group and acknowledges postdoctoral
 875 fellowship support from the Spanish “Juan de la Cierva Incorporación (IJC2020)” program (MICINN,
 876 Spain). The Institut Català de Paleoecologia Humana i Evolució Social (IPHES-CERCA) received financial
 877 support from the Spanish Ministry of Science and Innovation through the “María de Maeztu” program
 878 for Units of Excellence (CEX2019-000945-M). This paper is also a contribution to the "HumAN and
 879 climAtic iMPlicatioNs of palaEoecological changeS in large ISlands in the central Mediterranean
 880 (ANAMNESIS, Code: RM1221816B963D12, University of Roma La Sapienza)" programme directed by
 881 Federico Di Rita. The authors also acknowledge Pr. V. Pascucci and an anonymous reviewer for their
 882 fruitful comments. Finally, we would like to thank Rachel Mackie for improving the English.

883

884 **References**

885 Archivio di stato di Genova, 1639. Cornelius de Witt: source archivistique, fond Corsica, 948, Relatione del bosco
 886 di Aitona del Capitano Olandese.

887
 888 Bassetti MA, Berné S, Sicre, MA, Dennielou B, Alonso Y, Buscail R, Jalali B, Herbert B, Menniti C (2016)
 889 Holocene hydrological changes in the Rhône River (NW Mediterranean) as recorded in the marine mud belt.
 890 *Climate of the Past* 12: 1539-1553.

891
 892 Bengtsson L, Enell M (1986) Chemical analysis. In: Berglund BE (Ed.), *Handbook of Holocene Palaeoecology*
 893 *and Palaeohydrology*. John Wiley & Sons Ltd., Chichester, 423-451.

894
 895 Berger JF, Brochier JL, Vital J, Delhon C, Thiebault S (2007) Nouveau regard sur la dynamique des paysages et
 896 l'occupation humaine à l'Âge du bronze en moyenne vallée du Rhône. In : Mordant C, Richard H, Magny M (eds),
 897 *Environnements et cultures à l'âge du Bronze en Europe occidentale*. Actes du 129e colloque du CTHS, Besançon,
 898 avril 2004, Editions du CTHS, Documents Préhistoriques, 21, 260-283.

899
 900 Biserni G and van Geel B (2005) Reconstruction of Holocene palaeoenvironment and sedimentation history of the
 901 Ombrone alluvial plain (South Tuscany, Italy). *Review of Palaeobotany and Palynology* 136(1-2): 16-28.

902
 903 Blaauw M (2010) Methods and code for ‘classical’ age-modelling of radiocarbon sequences. *Quat Geochronol* 5
 904 : 512–518.

905
 906 Bond G, Showers W, Cheseby M, Lotti R, Almasi P, deMenocal PB, Priore P, Cullen H, Hajdas I, Bonani G (1997)
 907 A pervasive millennial-scale cycle in North Atlantic Holocene and glacial climates. *Science* 278 : 1257–1265.

908
 909 Brisset E, Burjachs F, Ballesteros Navarro BJ, Fernández-López J (2018). Socioecological adaptation to Early-
 910 Holocene sea-level rise in the western Mediterranean. *Global and Planetary Change* 169: 56-167.

911
 912 Brückner H, Vött A, Schriever A, Handl M (2005) Holocene delta progradation in the eastern Mediterranean— case
 913 studies in their historical context. *Méditerranée* 104 : 95-106.

914
 915 Burjachs F, Jones SE, Giralt S, de Pablo JFL (2016) Lateglacial to Early Holocene recursive aridity events in the
 916 SE Mediterranean Iberian Peninsula: The Salines playa lake case study. *Quaternary International* 403: 187-200.

917
 918
 919 Burjachs F, Pérez-Obiol R, Picornell-Gelabert L, Revelles J, Servera-Vives G, Expósito I, Yll EI (2017) Overview
 920 of environmental changes and human colonization in the Balearic Islands (Western Mediterranean) and their
 921 impacts on vegetation composition during the Holocene. *Journal of Archaeological Science: Reports*: 12: 845-859.

922
 923 Buurman P, Pape T, Muggler CC (1996) Laser grain-size determination in soil genetic studies: practical problems.
 924 *Soil Sci.* 162 (3) : 211–218.

925
 926 Cacho I, Grimalt JO, Canals M, Sbaiffi L, Shackleton NJ, Schoenfeld J, Zahn R (2001) Variability of the western
 927 Mediterranean Sea surface temperature during the last 25,000 years and its connection with the Northern
 928 Hemisphere climatic changes. *Paleoceanography* 16 (1): 40-52.

- 929
930 Català A, Cacho I, Frigola J, Pena L D, Lirer F (2019). Holocene hydrography evolution in the Alboran Sea: a
931 multi-record and multi-proxy comparison. *Climate of the Past* 15(3) : 927-942.
932
933 Cibecchini F, Dieulefet G (2014) Le site de mouillage de Girolata (Corse). *Archéothème* 32 : 16-19.
934
935 Currás A, Ghilardi M, Peche-Quilichini K, Fagel N, Vacchi M, Delanghe D, Contreras D, Vella C, Ottaviani, JC
936 (2017). Reconstructing past landscapes of the eastern plain of Corsica (NW Mediterranean) during the last 6000
937 years based on molluscan, sedimentological and palynological analyses. *J. Archaeol. Sci.: Report* 12: 755-769.
938
939 Dean Jr. W.E (1974) Determination of carbonate and organic matter in calcareous sediments and sedimentary
940 rocks by loss on ignition: comparison with other methods. *J. Sediment. Petrol.* 44: 242-248.
941
942 Della Grossa G. et Montegiani P. 2016. *Giovanni Della Grossa, Pier'Antonio Montegiani. Chronique de la Corse*
943 *des origines à 1546. Introduction, traduction et notes d'Antoine-Marie Graziani, Ajaccio, Piazzola, 592-593.*
944
945 Di Rita F, Magri D (2012) An overview of the Holocene vegetation history from the central Mediterranean coasts.
946 *J. Mediterr. Earth Sci.* 4: 35-52.
947
948 Di Rita F, Ghilardi M, Fagel N, Vacchi M, Warichet F, Delanghe D, Sicurani J, Martinet L, Robresco S (2022a).
949 Natural and anthropogenic dynamics of the coastal environment in north western Corsica (Western Mediterranean)
950 over the past six millennia. *Quaternary Science Reviews* 278: 107372
951
952 Di Rita F, Michelangeli F, Celant A, Magri D (2022b) Sign-switching ecological changes in the Mediterranean
953 basin at 4.2 ka BP. *Global and Planetary Change* 208: 103713.
954
955 Emberger L (1930) La végétation de la région méditerranéenne: essai d'une classification des groupements
956 végétaux. *Revue de Botanique*, Librairie générale de l'enseignement, 503: 642-662 ; 504:705-721.
957
958 Faegri K, Iversen J (1989) *Text-book of modern pollen analysis*. Ejnar Munksgaard. Copenhagen.
959
960 Fletcher WJ, Debret M, Goñi MFS (2013) Mid-Holocene emergence of a low-frequency millennial oscillation in
961 western Mediterranean climate: Implications for past dynamics of the North Atlantic atmospheric westerlies. *The*
962 *Holocene* 23 (2) : 153-166.
963
964 Fontana A, Vinci G, Tasca G, Mozzi P, Vacchi M, Bivi G, Salvador S, Rossato S, Antonioli F, Asioli A, Bresolin
965 M, Di Mario F, Hajdas I (2017) Lagoonal settlements and relative sea level during bronze age in northern Adriatic:
966 Geoarchaeological evidence and paleogeographic constraints. *Quat. Int.* : 439 : 17-36.
967
968 Galop D, Carozza L, Marembert F, Bal MC (2007) Activités agropastorales et climat durant l'Âge du Bronze dans
969 les Pyrénées : l'état de la question à la lumière des données environnementales et archéologiques. In : Mordant C,
970 Richard H, Magny M. (eds) *Environnements et cultures à l'âge du Bronze en Europe occidentale*. Actes du 129e
971 colloque du CTHS, Besançon, avril 2004, Editions du CTHS, Documents Préhistoriques, 21, 107-119.
972
973 Ghilardi M (2021) Geoarchaeology: where Geosciences meet with Humanities to reconstruct past
974 Humans/Environment interactions. An application to the coastal areas of the largest Mediterranean islands.
975 *Applied Sciences* 11 (10): 4480.
976
977 Ghilardi M (2020) *Lagunes et marais littoraux de Corse. De la Préhistoire à nos jours*. Collec. Orma : la Corse
978 archéologique, Editions ARAC, 5 : 105 p.
979
980 Ghilardi M, Istria D, Currás A, Vacchi M, Contreras D, Vella C, Dussouillez P, Crest Y, Collet M, Guiter F,
981 Delanghe D. (2017a) Reconstructing the landscape evolution and the human occupation of the Lower Sagone
982 River (Western Corsica, France) from the Bronze Age to the Medieval period. In: Ghilardi M and Lespez L (eds),
983 *Geoarchaeology of the Mediterranean islands*, Journal of Archaeological Science: Reports, 12: 741-754.
984
985 Ghilardi M, Delanghe D, Demory F, Leandri F, Pêche-Quilichini K, Vacchi M, Vella MA, Rossi V, Robresco S
986 (2017b) Enregistrements d'événements extrêmes et évolution des paysages dans les basses vallées fluviales du
987 Taravo et du Sagone (Corse occidentale, France) au cours de l'âge du Bronze moyen à final : une perspective
988 géoarchéologique. *Géomorphologie, Relief, Processus et Environnement* 23(1) : 15-35.

- 1
2
3 989
4 990 Giaime M, Salem A, Wang Y, Zhao X, Liu Y, Chen J, Sun A, Abu Shama AM, Elhossainy M, Morhange C, Chen
5 991 Z (2022). Holocene evolution and signature of environmental change of the Burullus lagoon (Nile Delta)
6 992 deciphered from a long sediment record. *Palaeogeography, Palaeoclimatology, Palaeoecology* 590 : 110861.
7 993
8 994 Girard M, Renault-Miskovsky J (1969) Nouvelles techniques de préparation en Palynologie appliqués à trois
9 995 sédiments du Quaternaire final de l'Abri Cornille (Istres -Bouches du Rhône). *Bulletin AFEQ* 4: 275-284.
10 996
11 997 Giraudi C (2011) The sediments of the "Stagno di Maccarese" marsh (Tiber river delta, central Italy): A late-
12 998 Holocene record of natural and human-induced environmental changes. *The Holocene* 21(8): 1233-1243.
13 999
14 1000 Giraudi C, Tata C, Paroli L (2009) Late Holocene evolution of the Tiber river delta and geoarchaeology of Claudius
15 1001 and Trajan harbour, Rome. *Geoarchaeology* 24(3) : 371-382.
16 1002
17 1003 Giustiniani A., 1993. *Augustino Giustiniani. Description de la Corse. Préface, notes et traduction d'Antoine-*
18 1004 *Marie Graziani.* Ajaccio, Piazzola, coll. Source de l'Histoire de la Corse, Textes et documents.
19 1005
20 1006 Goeury C, de Beaulieu JL (1979) À propos de la concentration du pollen à l'aide de la liqueur de Thoulet dans les
21 1007 sédiments minéraux. *Pollen et Spores* XXI (1-2): 239- 251.
22 1008
23 1009 Graziani A.M., 2004. *La forêt en Corse. Des origines à nos jours*, Archives départementales de la Corse-du-Sud,
24 1010 Ajaccio, 59 p.
25 1011
26 1012 Grimm EC (1987) CONISS: a Fortran 77 program for stratigraphically constrained cluster analysis by the method
27 1013 of incremental sum of squares. *Comput.Geosci.* 13:13-55.
28 1014
29 1015 Grimm EC (1991-2011). Tilia, Tilia-Graph and TGView. Illinois State Museum, Springfield,
30 1016 <http://museum.state.il.us/pub/grimm/tilia/>
31 1017
32 1018 Huser A, Ben Chaba L, Abel V, Sivan O (2017). *Le fortin de Girolata. Une tour isolée devenue fortin, fouille et*
33 1019 *étude du bâti.* Rapport final de synthèse (INRAP), Nîmes, 444pp.
34 1020
35 1021 Lestienne M, Jouffroy-Bapicot I, Leysenne D, Sabatier P, Debret M, Albertini PJ, Colombaroli D, Didier J, Hély
36 1022 C, Vannière B (2020). Fires and human activities as key factors in the high diversity of Corsican vegetation. *The*
37 1023 *Holocene* 30: 244-257.
38 1024
39 1025 Leveau P (1990) L'organisation de l'espace agricole en Afrique à l'époque romaine. In : L'Afrique dans l'Occident
40 1026 romain (1er siècle av. J.-C. - IVe siècle ap. J.-C.). Actes du colloque de Rome (3-5 décembre 1987) Rome : École
41 1027 Française de Rome, *Publications de l'École française de Rome*, 134 : 129-141.
42 1028
43 1029 Leys B, Finsinger W, Carcaillet C (2014) Historical range of fire frequency is not the Achilles' heel of the Corsican
44 1030 black pine ecosystem. *Journal of Ecology* 102(2): 381–395.
45 1031
46 1032 Leys B, Curt T, Elkin C (2018) Mosaic landscape pattern explains vegetation resistance to high fire frequency in
47 1033 Corsica over the last six millennia. *Int J Earth Sci Geophys* 4: 1-7.
48 1034
49 1035 Lombard M (1959) Un problème cartographié : le bois dans la Méditerranée musulmane: VIIe-XIe siècles. Armand
50 1036 Colin, *Annales Economie-Sociétés-Civilisations* 2 : 234-254.
51 1037
52 1038 Lombard M (1972) Espaces et réseaux du haut moyen âge, Mouton, Paris : École des Hautes Études en Sciences
53 1039 Sociales, coll. « *Le savoir historique 2* » : 162-165.
54 1040
55 1041 López-Belzunce M, Blázquez AM, Carmona P, Ruiz JM (2020). Multi proxy analysis for reconstructing the late
56 1042 Holocene evolution of a Mediterranean Coastal Lagoon: Environmental variables within foraminiferal
57 1043 assemblages. *Catena* 187: 104333.
58 1044
59 1045 López-Sáez JA, Pérez-Díaz S, Galop D, Alba-Sánchez F, Abel-Schaad D (2015) A Late Antique vegetation history
60 1046 of the Western Mediterranean in context. *Late Antique Archaeology* 11(1): 83-104.
61 1047

- 1
2
3 1048 Ljungqvist F.K. (2010) A new reconstruction of temperature variability in the extra-tropical northern hemisphere
4 1049 during the last two millennia. *Geografiska Annaler : Series A, Physical Geography* 92(3), 339-351.
5 1050
- 6 1051 Magny M (2004) Holocene climate variability as reflected by mid-European lake level fluctuations and its probable
7 1052 impact on prehistoric human settlements. *Quaternary International* 113: 65-79.
8 1053
- 9 1054 Magny M, de Beaulieu JL, Drescher-Schneider R, Vanni re B, Walter-Simonnet AV, Miras Y, Millet L, Bossuet
10 1055 G, Peyron O, Brugiapaglia E, Leroux A (2007). Holocene climate changes in the central Mediterranean as recorded
11 1056 by lake-level fluctuations at Lake Accesa (Tuscany, Italy). *Quaternary Science Reviews* 26(13-14): 1736-1758.
12 1057
- 13 1058 Marco-Barba J, Holmes JA, Mesquita-Joanes F, Miracle MR (2013) The influence of climate and sea-level change
14 1059 on the Holocene evolution of a Mediterranean coastal lagoon: Evidence from ostracod palaeoecology and
15 1060 geochemistry. *Geobios* 46(5): 409-421.
16 1061
- 17 1062 Marco-Barba J, Burjachs F, Reed JM, Santisteban C, Usera JM, Alberola C, Exposito I, Guillem J, Patchett F,
18 1063 Mesquita-Joanes F, Miracle MR (2019) Mid-holocene and historical palaeoecology of the albufera de Val ncia
19 1064 Coastal Lagoon. *Limnetica* 38 : 353-389.
20 1065
- 21 1066 Mary JB (2013) *Analyses et approches typologiques de l'occupation protohistorique et antique de la r gion ouest*
22 1067 *de la Corse*. Master thesis, University of Aix-Marseille, 160 p.
23 1068
- 24 1069 Mary JB (2014a) *Nouveau regard sur les fortifications de l' ge du Fer au changement d' re : le cas de la fa ade*
25 1070 *centre occidentale*. Master Thesis, University of Aix-Marseille, 189 p.
26 1071
- 27 1072 Mary JB (2014b) *Prospection-inventaire des communes de Partinellu, Ota et Osani*. Rapport final de Synth se,
28 1073 Service R gional de l'Arch ologie de Corse, 10-27.
29 1074
- 30 1075 Mary JB (2014c) * tude du mobilier c ramique du fortin de Girolata*. In : le fortin de Girolata, Rapport d'op ration
31 1076 (INRAP), N mes, 104-111.
32 1077
- 33 1078 Mary JB (2018)  tudes et constat pr liminaires des implantations fortifi es de Corse, du second  ge du Fer au
34 1079 changement d' re. Le cas de la r gion centre-ouest de la Corse. In : *insularity and identity in the Roman*
35 1080 *Mediterranean*, Oxbow books :165-198.
36 1081
- 37 1082 Mary JB (2021) *Prospection-th matique avec sondages d' valuation, 2020. Communes de Coggia, Vico, Carg se,*
38 1083 *Piana, Ota, Serierra, Partinellu, Osani (Corse-du-Sud)*. Rapport final de synth se, Service r gional de
39 1084 l'arch ologie de Corse, 164 p.
40 1085
- 41 1086 Mary JB (2022) * tude du mobilier c ramique du fortin de Girolata*. In : le fortin de Girolata, Rapport d'op ration
42 1087 (INRAP), N mes, 127-137.
43 1088
- 44 1089 Mayewski PA, Rohling EE, Stager JC, Karlen W, Maasch KA, Meeker LD, Meyerson EA, Gasse F, Van Kreveld
45 1090 S, Holmgren K, Lee-Thorp J, Rosqvist G, Rack F, Staubwasser M, Schneider RR, Steig EJ (2004) Holocene
46 1091 climate variability. *Quaternary Research* 62 (3): 243-255.
47 1092
- 48 1093 Melis RT, Depalmas A, Di Rita F, Montis F, Vacchi M (2017) Mid to late Holocene environmental changes along
49 1094 the coast of western Sardinia (Mediterranean Sea). *Global and Planetary Change* 155 : 29-41.
50 1095
- 51 1096 Pascucci V., De Falco G., Del Vais C., Sanna I., Melis R.T., Andreucci S. (2018) Climate changes and human
52 1097 impact on the Mistras coastal barrier system (W Sardinia, Italy), *Marine Geology* 395 : 271-284.
53 1098
- 54 1099 P che-Quilichini K (2015a) Les torre. Enigmatiques tours de l' ge du Bronze. *Archaeologia* 528 : 49-55.
55 1100
- 56 1101 P che-Quilichini K (2015b) L' ge du Bronze corse. L' mergence d'une  lite guerri re. *Dossiers d'Arch ologie*
57 1102 370: 24-29.
58 1103
- 59 1104 P res JM (1982) Major benthic assemblages. In: Kinne O (ed), *Marine Ecology*, Part 1, vol. 5. Wiley, Chichester,
60 1105 pp. 373-522.
61 1106

- 1
2
3 1107 Péres JM, Picard J (1964). Nouveau manuel de Bionomie benthique de la Mer Méditerranée. *Recueil des Travaux*
4 1108 *de la station Marine d'Endoume*31 (47) : 5-137.
5 1109
6 1110 Petti Balbi G (1976) *Genova nel trecento*, 97-98. Istituto storico italiano per il medio evo, Roma, 195 p.
7 1111
8 1112 Poher Y, Ponel P, Médail F, Andrieu-Ponel V, Guiter F (2017) Holocene environmental history of a small
9 1113 Mediterranean island in response to sea-level changes, climate and human impact. *Palaeogeography,*
10 1114 *Palaeoclimatology, Palaeoecology* 465: 247-263. Part A.
11 1115
12 1116 Pranzini E (2001) Updrift river mouth migration on cusped deltas : two examples from the coast of Tuscany
13 1117 (Italy). *Geomorphology* 38: 125-132.
14 1118
15 1119 Rasmussen SO, Bigler M, Blockley SP, Blunier T, Buchardt SL, Clausen HB, Cvijanovic I, Dahl-Jensen D,
16 1120 Johnsen SJ, Fischer H, Gkinis V, Guillevic M, Hoek WZ, Lowe JJ, Pedro JB, Popp T, Seierstad IK, Steffensen JP,
17 1121 Svensson AM, Vallelonga P, Vinther BM, Walker MJC, Wheatley JJ, Winstrup M (2014) A stratigraphic
18 1122 framework for abrupt climatic changes during the Last Glacial period based on three synchronized Greenland ice-
19 1123 core records: refining and extending the INTIMATE event stratigraphy. *Quat. Sci. Rev.* 106: 14–28.
20 1124
21 1125 Reille M (1992a) New pollen-analytical researches in Corsica: the problem of *Quercus ilex* L. and *Erica arborea*
22 1126 L., the origin of *Pinus halepensis* Miller forests. *New Phytologist* 122: 359-378.
23 1127
24 1128 Reille M(1992b) *Pollen et spores d'Europe et d'Afrique du nord, Laboratoire de botanique historique et*
25 1129 *palynologie*. Marseille, France: URA, CNRS, Laboratoire de Botanique Historique et Palynologie.
26 1130
27 1131 Reille M (1988) Recherches pollenanalytiques dans le cap Corse: analyse pollinique du marais de Barcaggio. *Trav.*
28 1132 *Sci. du Parc Nat. régional des Réserves Nat. Corse* 18 : 77-92.
29 1133
30 1134 Reille M (1984) Origine de la végétation actuelle de la Corse sud-orientale; analyse pollinique de cinq marais
31 1135 côtiers. *Pollen et Spores* 26 : 43-60.
32 1136
33 1137 Reille M (1975) *Contribution pollenanalytique à l'histoire tardiglaciaire et holocène de la végétation de la*
34 1138 *montagne corse*. Thèse de Doctorat des sciences, Aix-Marseille III.
35 1139
36 1140 Reimer PJ and McCormac FG (2002) Marine radiocarbon reservoir corrections for the Mediterranean and Aegean
37 1141 Seas. *Radiocarbon* 44 (1) :, 159-166.
38 1142
39 1143 Reimer P, Austin WEN, Bard E, Bayliss A, Blackwell PG, Bronk Ramsey C, Butzin M, Cheng H, Edwards RL,
40 1144 Friedrich M, Grootes PM, Guilderson TP, Hajdas I, Heaton TJ, Hogg AG, Hughen KA, Kromer B, Manning SW,
41 1145 Muscheler R, Palmer JG, Pearson C, van der Plicht J, Reimer RW, Richards DA, Scott EM, Southon JR, Turney
42 1146 CSM, Wacker L, Adolphi F, Büntgen U, Capano M, Fahrni S, Fogtmann-Schulz A, Friedrich R, Köhler P, Kudsk
43 1147 S, Miyake F, Olsen J, Reinig F, Sakamoto M, Sookdeon A, Talamo S (2020)The IntCal20 Northern Hemisphere
44 1148 radiocarbon age calibration curve (0-55 calkBP). *Radiocarbon* 62(4):725-757.
45 1149
46 1150 Revelles J, Ghilardi M, Vacchi M, Rossi V, Currás A, López-Bultò O, Brkojewitsch G (2019) Coastal landscape
47 1151 evolution of Corsica: palaeoenvironments, vegetation history and human impacts since the Early Neolithic period,
48 1152 *Quaternary Science Reviews*, 105993.
49 1153
50 1154 Revelles J, Burjachs F, Van Geel B (2016) Pollen and non-pollen palynomorphs from the Early Neolithic
51 1155 settlement of La Draga (Girona, Spain). *Review of Palaeobotany and Palynology* 225: 1-20.
52 1156
53 1157 Rotta MP and Cancellieri JA (2001) *De la nature à l'histoire; les forêts de la Corse*. Ed. Alain Piazzola, 159 p.
54 1158
55 1159 Sabatier P, Dézileau L, Barbier M, Raynal O, Lofi J, Briquieu L, Condomines M, Bouchette F, Certain R, Van
56 1160 Grafenstein U, Jorda C, Blanchemanche P (2010). Late-Holocene evolution of a coastal lagoon in the Gulf of
57 1161 Lions (South of France). *Bulletin de la Société géologique de France* 181 (1) : 27-36.
58 1162
59 1163 Servera-Vives G, Riera S, Picornell-Gelabert L, Moffa-Sánchez P, Llergo Y, Garcia A, ... &Trías MC (2018). The
60 1164 onset of islandscapes in the Balearic Islands: A study-case of Addaia (northern Minorca, Spain). *Palaeogeography,*
61 1165 *Palaeoclimatology, Palaeoecology*498: 9-23.
62 1166

- 1
2
3 1167 Shom - Collectivité de Corse - Dreal Corse (2020)*Litto3D*,
4 1168 https://dx.doi.org/10.17183/L3D_MAR_CORSE_2017_2018
5 1169
6 1170 Siani G, Paterne M, Arnold M, Bard E, Metivie B, Tisnerat N, Bassinot F (2000) Radiocarbon reservoir ages in
7 1171 the Mediterranean Sea and Black Sea. *Radiocarbon* 42 : 271–280.
8 1172
9 1173 Stuiver M and Reimer P.J (1993) Calib software v. 8.2, *Radiocarbon* 35 : 215-230.
10 1174
11 1175 Tramoni P, d'Anna A (2016) Le Néolithique moyen de la Corse revisité : nouvelles données, nouvelles
12 1176 perceptions. In : Perrin T, Chambon P, Gibaja JF, Goude G(eds), *Le Chasséen, des Chasséens... Retour sur une*
13 1177 *culture nationale et ses parallèles, Sepulcres de fossa, Cortaillod, Lagozza*. Actes du colloque international tenu
14 1178 à Paris (France) du 18 au 20 novembre 2014, Archives d'Ecologie Préhistorique, 59-72.
15 1179
16 1180 Vacchi M, Marriner N, Morhange C, Spada G, Fontana A, Rovere A(2016) Multiproxy assessment of Holocene
17 1181 relative sea-level changes in the western Mediterranean: sea-level variability and improvements in the definition
18 1182 of the isostatic signal. *Earth Sci. Rev.* 155: 172-197.
19 1183
20 1184 Vacchi M, Ghilardi M, Melis RT, Spada G, Giaime M, Marriner N, Lorscheid T, Morhange C, Burjachs F, Rovere
21 1185 A (2018) New relative sea-level insights into the isostatic history of the Western Mediterranean. *Quat. Sci. Rev.*
22 1186 201: 396e408.
23 1187
24 1188 Van Geel B (1978) A palaeoecological study of Holocene peat bog sections in Germany and The Netherlands.
25 1189 *Review of Palaeobotany and Palynology* 25: 1-120.
26 1190
27 1191 Van Geel B (2001) Non-pollen palynomorphs, en Smol, J.P., Birks, H.J.B., Last, W.M. (eds), Tracking
28 1192 Environmental Change using Lake Sediments: Terrestrial, Algal, and Siliceous Indicators, 3. Kluwer, Dordrecht,
29 1193 99–119.
30 1194
31 1195 Van Geel B, Mur LR, Ralska-Jasiewiczowa M (1994) Fossil akinetes of Aphanizomenon and Anabaena as
32 1196 indicators of medieval phosphate-eutrophication of Lake Goszcz (Central Poland). *Rev. Palaeobot. Palynol.* 83:
33 1197 97–105.
34 1198
35 1199 Van Geel B, Buurman J, Brinkkemper O, Schelvis J, Aptroot A, van Reenen G, Hakbijl T (2003) Environmental
36 1200 reconstruction of a Roman Period settlement site in Uitgeest (The Netherlands), with special reference to
37 1201 coprophilous fungi. *J. Archaeol.Sci.* 30: 873–883.
38 1202
39 1203 Vella MA, Andrieu-Ponel V, Cesari J, Leandri F, Peche-Quilichini K, Reille M, Poher Y, Demory F, Delanghe D,
40 1204 Ghilardi M, Ottaviani-Spella MD (2019) Early impact of agropastoral activities and climate on the littoral
41 1205 landscape of Corsica since mid-Holocene. *PLoS One* 14 (12) : e0226358.
42 1206
43 1207 Vellutini PJ, Orsini JB, Michon G, Brisset F, CocheméJJ(1985). *Carte géologique France (1/50000), feuille*
44 1208 *Galeria-Osani (1109)*. Orléans, BRGM.
45 1209
46 1210 Vellutini PJ, RossiP, Michon G, Hervé JY (1996) *Notice explicative, Carte géol. France (1/50000), feuille*
47 1211 *Galeria-Osani (1109)*. Orléans, BRGM, 109 p.
48 1212
49 1213 Wanner H, Solomina O, Grosjean M, Ritz SP, Jetel M (2011) Structure and origin of Holocene cold events. *Quat.*
50 1214 *Sci. Rev.* 30 (21–22): 3109-3123.
51 1215
52 1216 Yll EI, Perez-Obiol R, Pantaleon-Cano J, Roure J M (1997). Palynological evidence for climatic change and
53 1217 human activity during the Holocene on Minorca (Balearic Islands). *Quaternary Research*, 48(3): 339-347.
54 1218
55 1219
56 1220
57 1221
58 1222
59 1223
60 1224

Figure captions

1

2

3 1225 Figure 1 : Location map of the study area. Locator map: SF: Saint Florent. Digital Elevation Model is
 4 1226 derived from BDAlti data from IGN. Red stars indicate the location of the studied sites ;
 5 1227 Green circle : core drilled at Crovani pond (Di Rita et al., 2022a)

7 1228 Figure 2 : Geology, topography and archaeology of the Girolata-Novalla catchment. A : Geological
 8 1229 background and core location (geological data are derived from the 1 :50 000 scale map of
 9 1230 Osani ; Vellutini et al., 1985 and 1996). 1: Girolata ; 2 : A Chjesaccia ; 3 : Calanchelle ; 4 :
 10 1231 Novalla ; 5 : Girolata Fort ; 6 : modern shipwrecks (16th-18th centuries CE). B : View to the
 11 1232 south of the Girolata Plain and Gulf (source : J.B. Mary) with coring location and main
 12 1233 archaeological site.

15 1234 Figure 3 : Geology, topography and archaeology of the lower reaches of the Fangu catchment. A :
 16 1235 Geological background and core location (geological data are derived from the 1 :50 000
 17 1236 scale map of Osani ; Vellutini et al., 1985 and 1996). Yellow circle : site from the First phase
 18 1237 (1541-1553 cal. CE) of the Genoese administration of Corsica ; 1 : Galeria tower. B : Aerial
 19 1238 view to the south of the Fangu Estuary with coring and main archaeological site locations.

22 1239 Figure 4 : Depth/Age model for Fangu and Girolata 2 cores calculated with Clam 2.2 (Blaauw, 2010)
 23 1240 based on 10 and 6 radiocarbon dates, respectively. The model takes into account the 2σ -
 24 1241 confidence range of the calibrated ages. While linear interpolation fitted well to
 25 1242 radiocarbon data in the case of Girolata 2, the use of the smoothing spline method in the
 26 1243 Fangu sequence provided an age-depth curve closer to the radiocarbon data.

28 1244
 29 1245 Figure 5 :Chronostratigraphy of Girolata 1core

30 1246 Figure 6 :Chronostratigraphy of Girolata 2core

32 1247 Figure 7 :Chronostratigraphy of Fangu core

34 1248 Figure 8 : Pollen and NPP percentage diagrams for Girolata 2 core. White curves with depth bars show
 35 1249 exaggerated curves x2; white curves, exaggeration x5; dots represent occurrences of <1%.

37 1250 Figure 9 : Pollen and NPP percentage diagrams for Fangu core. White curves with depth bars show
 38 1251 exaggerated curves x2; white curves, exaggeration x5; dots represent occurrences of <1%.

40 1252 Figure 10 : Palaeogeographic reconstruction for the Girolata coastal plain for the last four millennia.

42 1253 Figure 11 : Diagram showing the evolution of arboreal pollen and anthropogenic indicators in Fangu,
 43 1254 Girolata 2, Crovani and Saint Florent cores for the last six millennia. Chronology of the cultural periods
 44 1255 for Prehistory and Protohistory is derived from Tramoni and D'Anna (2016). Categories: OVJC (*Olea*,
 45 1256 *Vitis*, *Juglans*, *Castanea*), Ruderals (*Rumex*, Brassicaceae, *Polygonum*, *Plantago*, *Urtica*), Coprophilous
 46 1257 fungi (*Sordaria*-t, *Sporormiella*, *Cercophora*-t, *Podospora*-t, *Delitschia*). Colour frames indicate the four
 47 1258 main phases of forest decline and grey frames indicate episodes of human impact without clear forest
 48 1259 decline. Bond events (Bond et al., 1997) and RCC events (Mayewski et al., 2004) are reported on the
 49 1260 graph.

52 1261 Figure 12 : Arboreal pollen (AP) evolution from the Iron Age onwards according to chronocultural
 53 1262 periods for the sites of Saint-Florent (Nebbiu) ; Crovani (Balagne) ; Fangu and Girolata (Filosorma). The
 54 1263 five major forest declines identified with palynology are highlighted with dashed grey bands; Event 2
 55 1264 alone is not documented in any known literary source. In the locator map : SF : Saint-Florent ; Cr. :
 56 1265 Crovani ; Fa. : Fangu ; Gi. : Girolata; Sa. : Sagone.

59 1266

60

1
2
3 1267 Table 1 : Borehole information.
4

5 1268 Table 2 : Radiocarbon dating results. Samples indicated by an * were rejected by the depth/age model
6 1269 calculation.
7

8 1270
9

10 1271 **Authors' contributions**

11 1272
12 1273 All authors have materially participated in the research project and article preparation, as follows.
13 1274 Conceptualization: MG, JR, FDR. Sediment collection: MG and JBM and LM. Methodology: MG, JR, FDR,
14 1275 DD. Formal analyses: MG, JR, JBM, CD, DD, and SR. Data collection: MG, JR, JBM, CD, DD. Results
15 1276 interpretation: MG, JR, JBM, FDR. Writing original draft: MG, JR. Contribution in interpreting results
16 1277 and writing the paper: MG, JR, FDR. Funding acquisition: MG, JBM.
17 1278

18 1278

19 1279

20 1280 **Declaration of competing interest**

21 1281

22 1282 The authors declare that they have no known competing financial interests or personal relationships
23 1283 that could have appeared to influence the work reported in this paper.
24
25
26
27
28
29
30
31
32
33
34
35
36
37
38
39
40
41
42
43
44
45
46
47
48
49
50
51
52
53
54
55
56
57
58
59
60

1
2
3
4
5
6
7
8
9
10
11
12
13
14
15
16
17
18
19
20
21
22
23
24
25
26
27
28
29
30
31
32
33
34
35
36
37
38
39
40
41
42
43
44
45
46

Site	Core id	Elevation amsl (in m, error : ± 0.1 m)	Length (in m)	X (WGS 84)	Y (WGS 84)	Easting (RGF/Lambert 93)	Northing (RGF/Lambert 93)
Girolata	Girolata 1	+ 0,88	3.15	8°36'51.95"E	42°21'2.67"N	1162962,28	6155430,50
	Girolata 2	+ 0,85	4.20	8°36'44.17"E	42°21'0.03"N	1162791,59	6155337,24
Fangu	Fangu	+ 0,70	4.20	8°39'34.07"E	42°25'7.83"N	1166123,87	6163257,70

Table 1 : Boreholes location. Elevation is derived from Litto3D survey (SHOM-Collectivité de Corse-DREAL, 2020)

Core id	Depth (in m)	Elevation amsl (in m)	Material	BP	Error ±	Cal ages	Lab. code
Girolata 1	1,66	-0,78	<i>Posidonia oceanica</i>	3280	30	1317-917 BCE	Poz-129246
	2,96	-2,08	<i>Posidonia oceanica</i>	3375	35	1424-1047 BCE	Poz-128585
Girolata 2	0,68	+0,17	Organic sediment	740	30	1226-1297 CE	Poz-129251
	0,96	-0,11	Organic sediment	1770	30	222-375 CE	Poz-129248
	1,33	-0,48	Charcoal	2455	30	754-415 BCE	Poz-129249
	2,66	-1,81	<i>Posidonia oceanica</i>	3125	30	1119-769 BCE	Poz-128586
	2,98	-2,13	Organic sediment	3115	30	1447-1286 BCE	Poz-129250
	4,1	-3,25	Charcoal	3495	35	1921-1696 BCE	Poz-128587
Fangu	0,48	+0,22	Charcoal	805	30	1179-1277 CE	Poz-141492
	0,6	+0,1	Charcoal	1215	30	689-889 CE	Poz-141286
	0,79	-0,09	Plant remains	130	30	1673-1942 CE*	Poz-145856
	1,74	-1,04	Charcoal	3550	30	2013-1772 BCE	Poz-145857
	1,87	-1,17	Charcoal	3655	35	2140-1929 BCE	Poz-141287
	2,35	-1,65	Charcoal	4050	35	2925-2693 BCE	Poz-144578
	2,71	-2,01	Charcoal	4755	35	3640-3376 BCE*	Poz-145858
	3,05	-2,35	Plant remains	4375	35	3092-2907 BCE	Poz-144494
	3,75	-3,05	Wood (<i>Pinus nigra/sylvestris</i>)	5000	40	3945-3653 BCE	Poz-145859
4,12	-3,42	Plant remains	4250	40	2672-2470 BCE*	Poz-144493	

Table 2 : Radiocarbon dating results

1
2
3
4
5
6
7
8
9
10
11
12
13
14
15
16
17
18
19
20
21
22
23
24
25
26
27
28
29
30
31
32
33
34
35
36
37
38
39
40
41
42
43
44
45
46
47
48
49
50
51
52
53
54
55
56
57
58
59
60

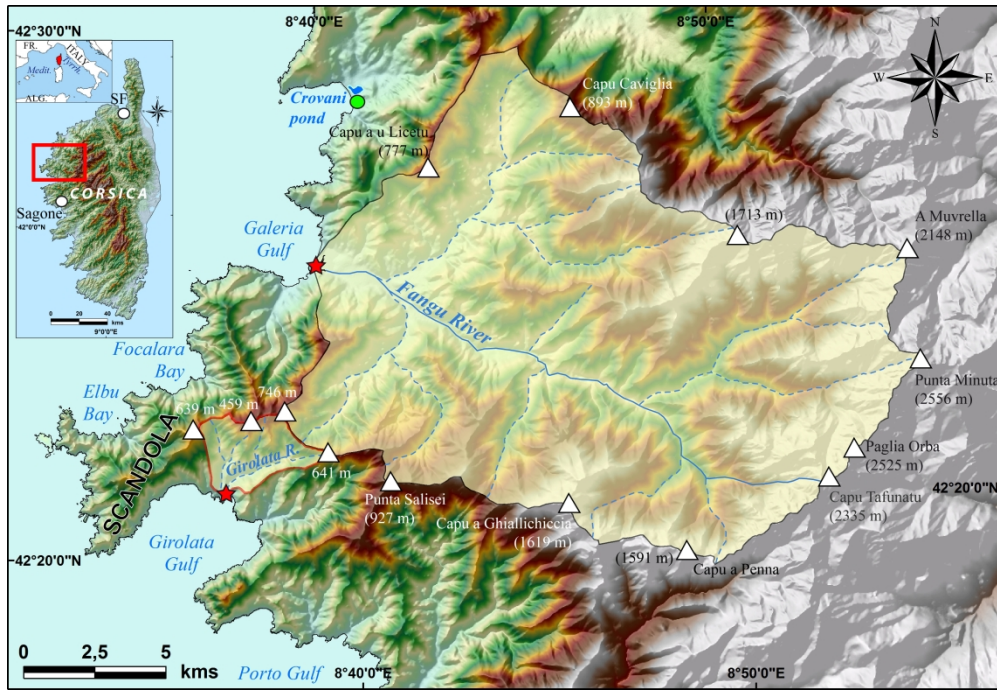


Figure 1: Location map of the study area. Locator map: SF: Saint Florent. Digital Elevation Model is derived from BDAlti data from IGN. Red stars indicate the location of the studied sites ; Green circle : core drilled at Crovani pond (Di Rita et al., 2022a)

293x200mm (300 x 300 DPI)

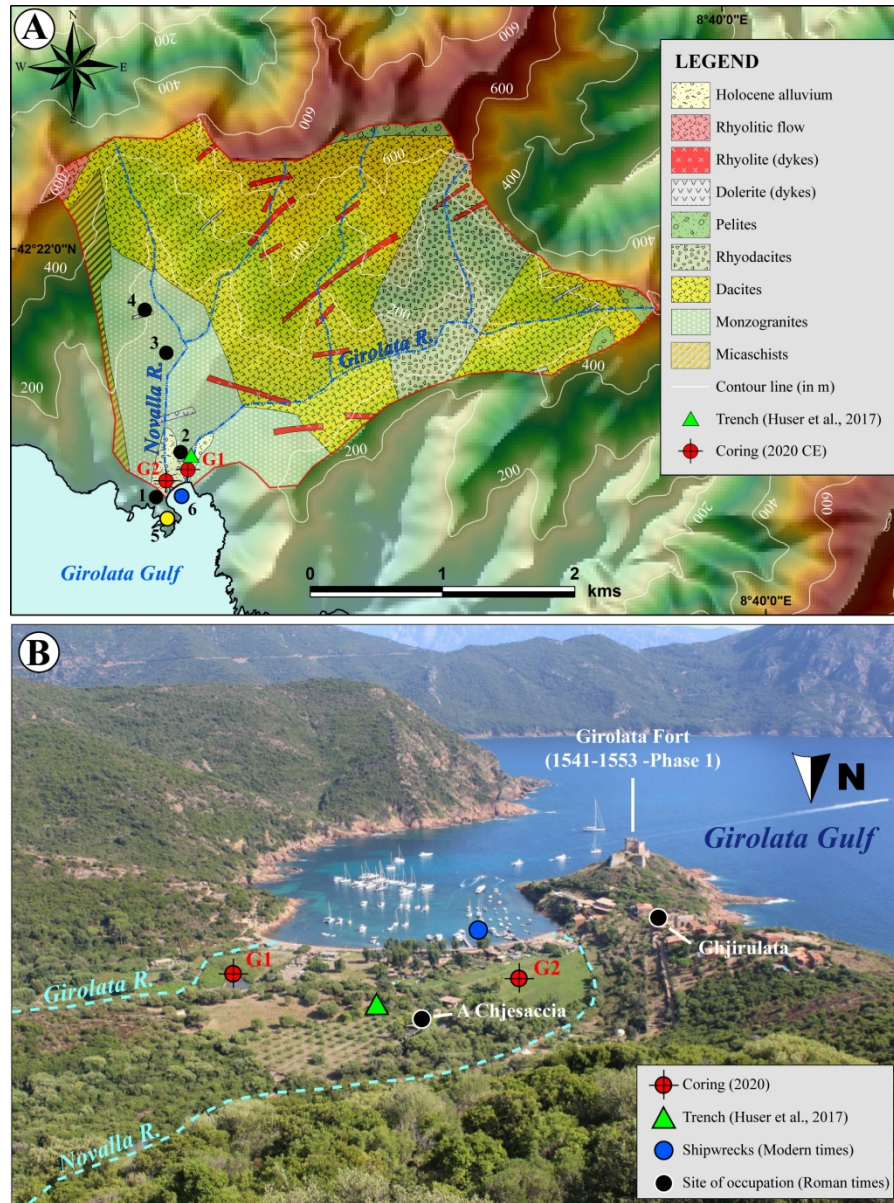


Figure 2 : Geology, topography and archaeology of the Girolata-Novalla catchment. A : Geological background and core location (geological data are derived from the 1 :50 000 scale map of Osani ; Vellutini et al., 1985 and 1996). 1 : Girolata ; 2 : A Chjesaccia ; 3 : Calanchelle ; 4 : Novalla ; 5 : Girolata Fort ; 6 : modern shipwrecks (16th-18th c. CE). B : View to the south of the Girolata Plain and Gulf (source : J.B. Mary) with coring location and main archaeological site.

204x276mm (300 x 300 DPI)

1
2
3
4
5
6
7
8
9
10
11
12
13
14
15
16
17
18
19
20
21
22
23
24
25
26
27
28
29
30
31
32
33
34
35
36
37
38
39
40
41
42
43
44
45
46
47
48
49
50
51
52
53
54
55
56
57
58
59
60

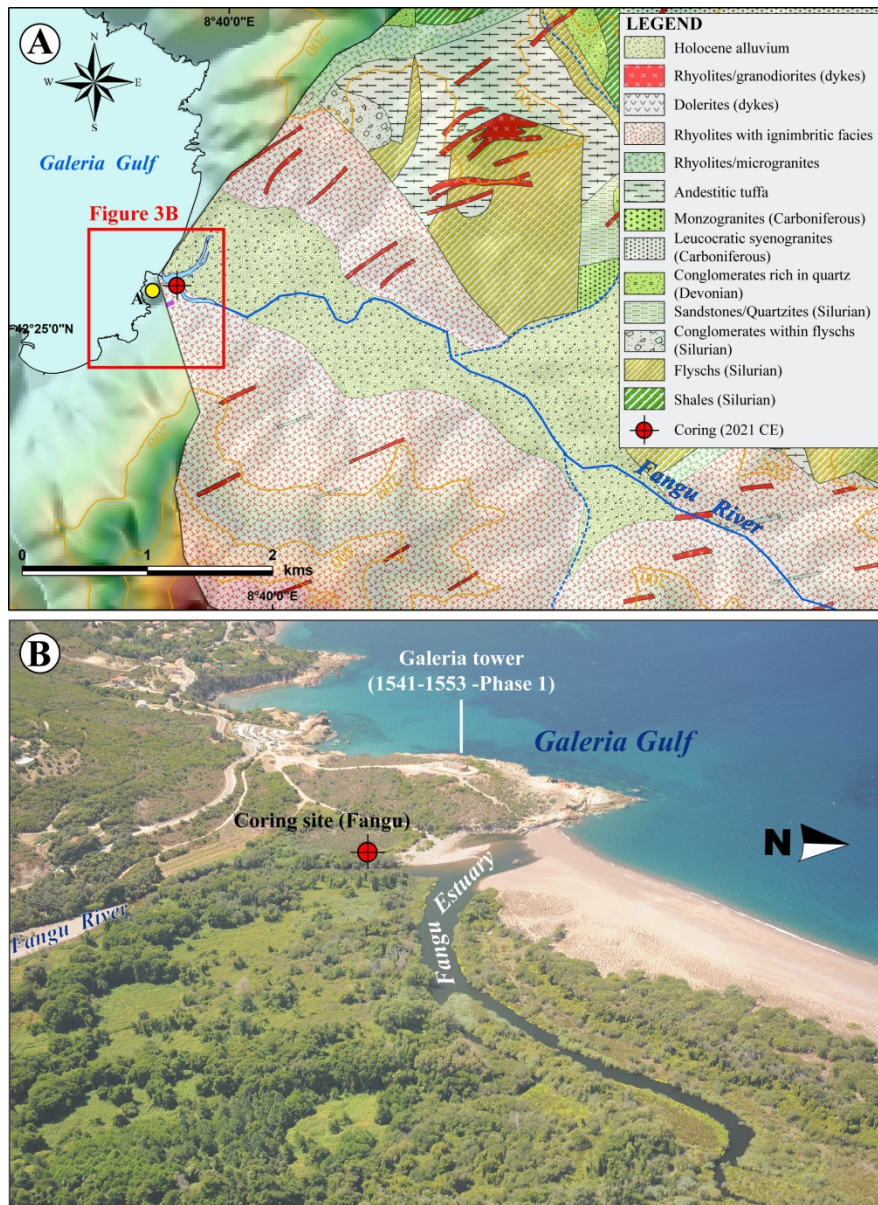


Figure 3 : Geology, topography and archaeology of the lower reaches of the Fangu catchment. A : Geological background and core location (geological data are derived from the 1 :50 000 scale map of Osani ; Vellutini et al., 1985 and 1996). Yellow circle : site from the First phase (1541-1553 cal. CE) of the Genoese administration of Corsica ; 1 : Galeria tower. B : Aerial view to the south of the Fangu Estuary with coring and main archaeological site locations.

205x279mm (300 x 300 DPI)

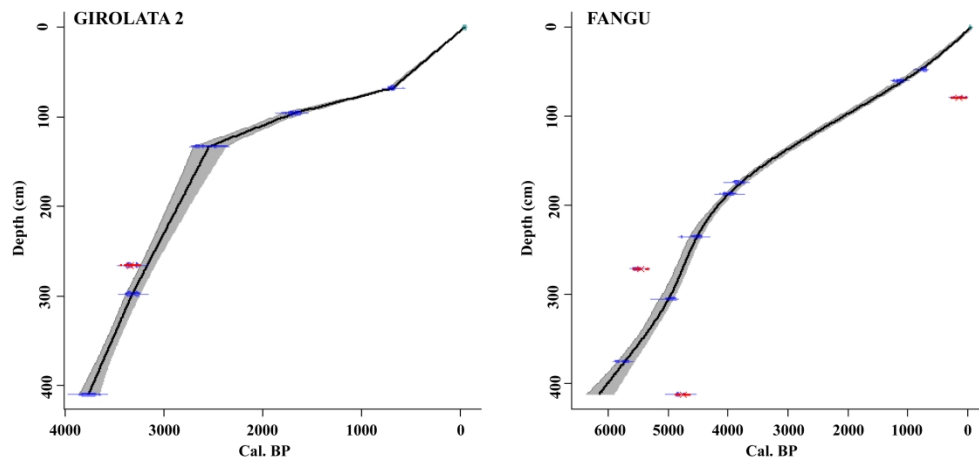


Figure 4: Depth/Age model for Fangu and Girolata 2 cores calculated with Clam 2.2 (Blaauw, 2010) based on 10 and 6 radiocarbon dates, respectively. The model takes into account the 2σ -confidence range of the calibrated ages. While linear interpolation fitted well to radiocarbon data in the case of Girolata 2, the use of the smoothing spline method in the Fangu sequence data provided an age-depth curve closer to the radiocarbon data.

267x127mm (300 x 300 DPI)

1
2
3
4
5
6
7
8
9
10
11
12
13
14
15
16
17
18
19
20
21
22
23
24
25
26
27
28
29
30
31
32
33
34
35
36
37
38
39
40
41
42
43
44
45
46
47
48
49
50
51
52
53
54
55
56
57
58
59
60

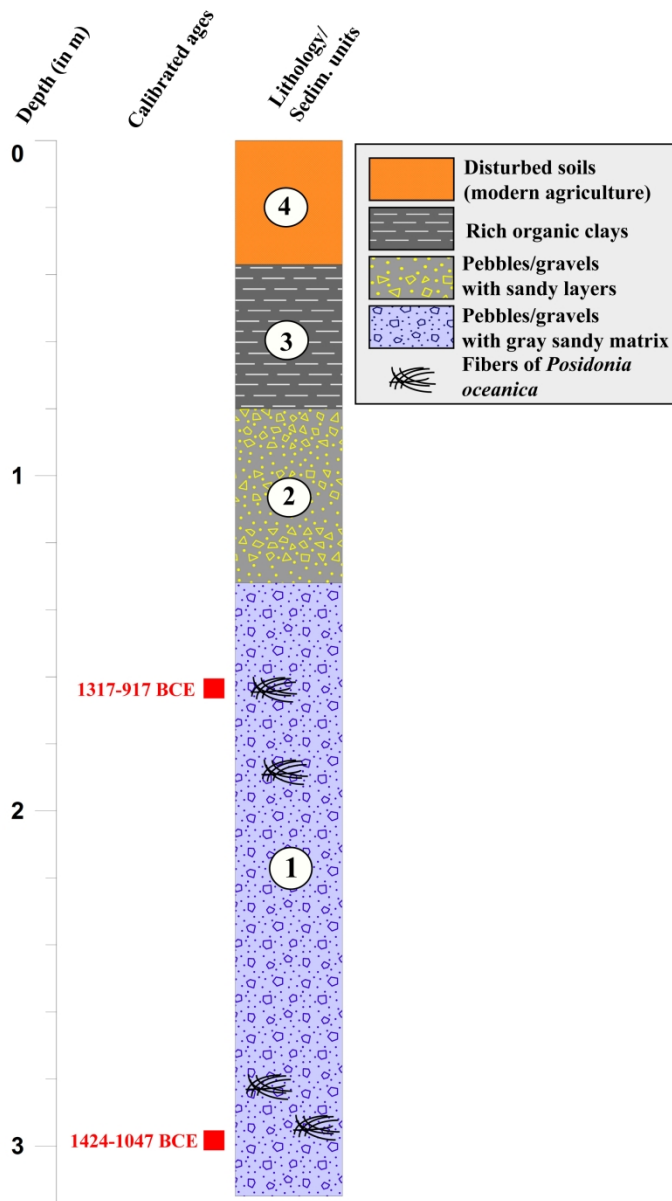


Figure 5 : Chronostratigraphy of Girolata 1 core

163x284mm (300 x 300 DPI)

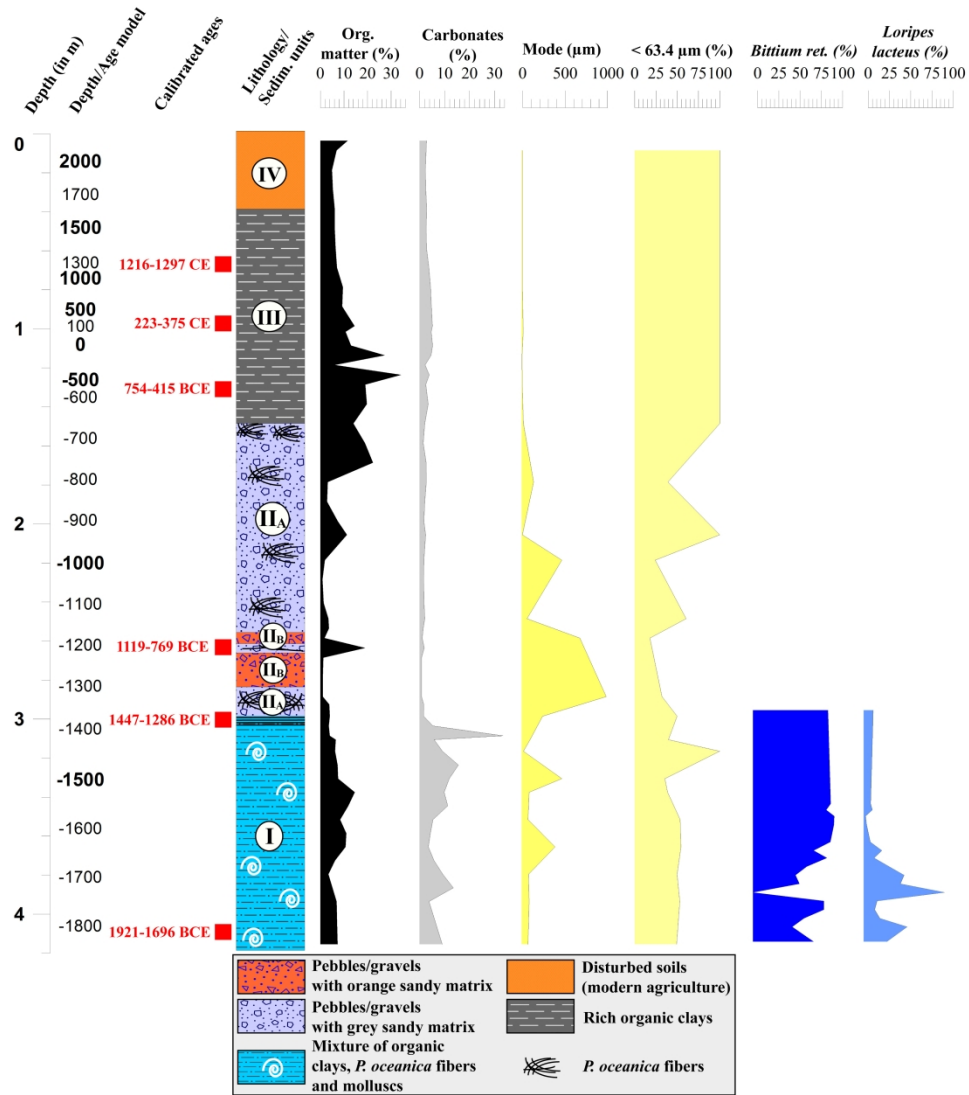


Figure 6 : Chronostratigraphy of Girolata 2core

298x325mm (300 x 300 DPI)

1
2
3
4
5
6
7
8
9
10
11
12
13
14
15
16
17
18
19
20
21
22
23
24
25
26
27
28
29
30
31
32
33
34
35
36
37
38
39
40
41
42
43
44
45
46
47
48
49
50
51
52
53
54
55
56
57
58
59
60

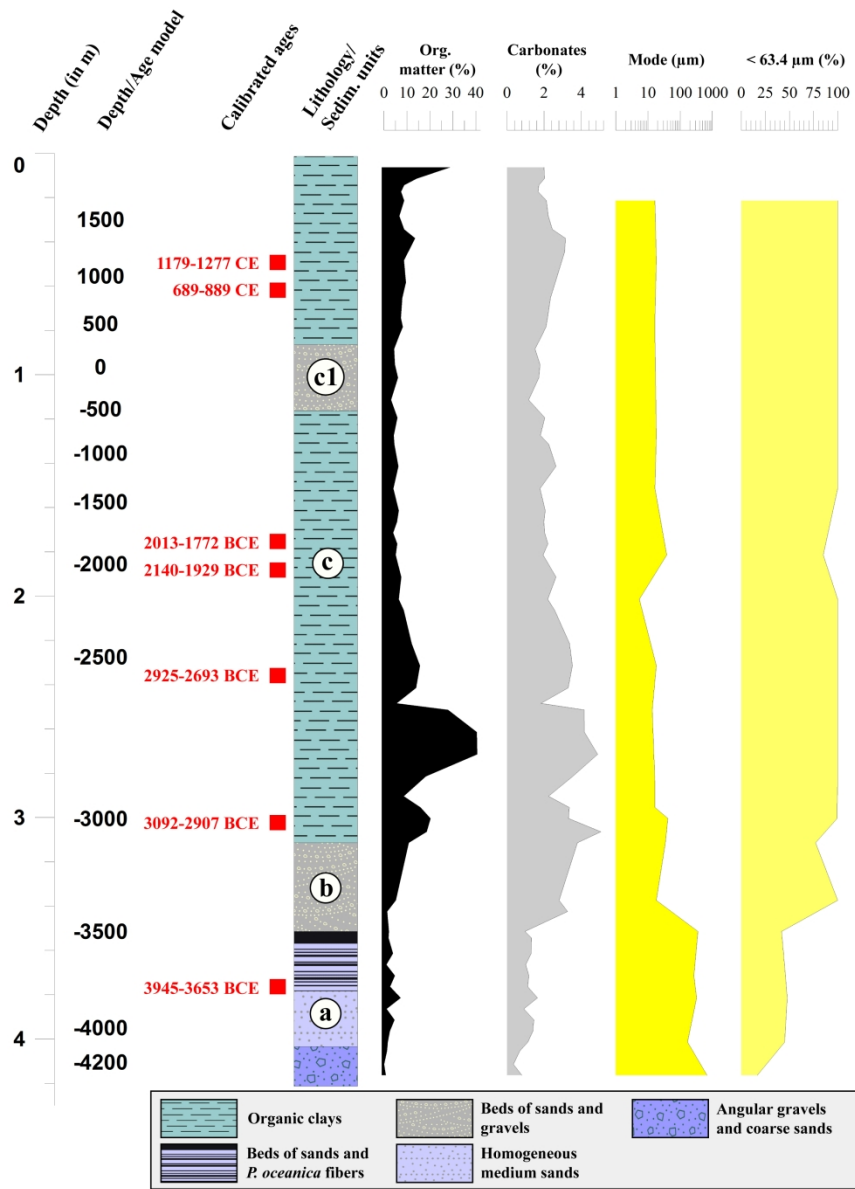


Figure 7 : Chronostratigraphy of Fangu core

225x315mm (300 x 300 DPI)

1
2
3
4
5
6
7
8
9
10
11
12
13
14
15
16
17
18
19
20
21
22
23
24
25
26
27
28
29
30
31
32
33
34
35
36
37
38
39
40
41
42
43
44
45
46
47
48
49
50
51
52
53
54
55
56
57
58
59
60

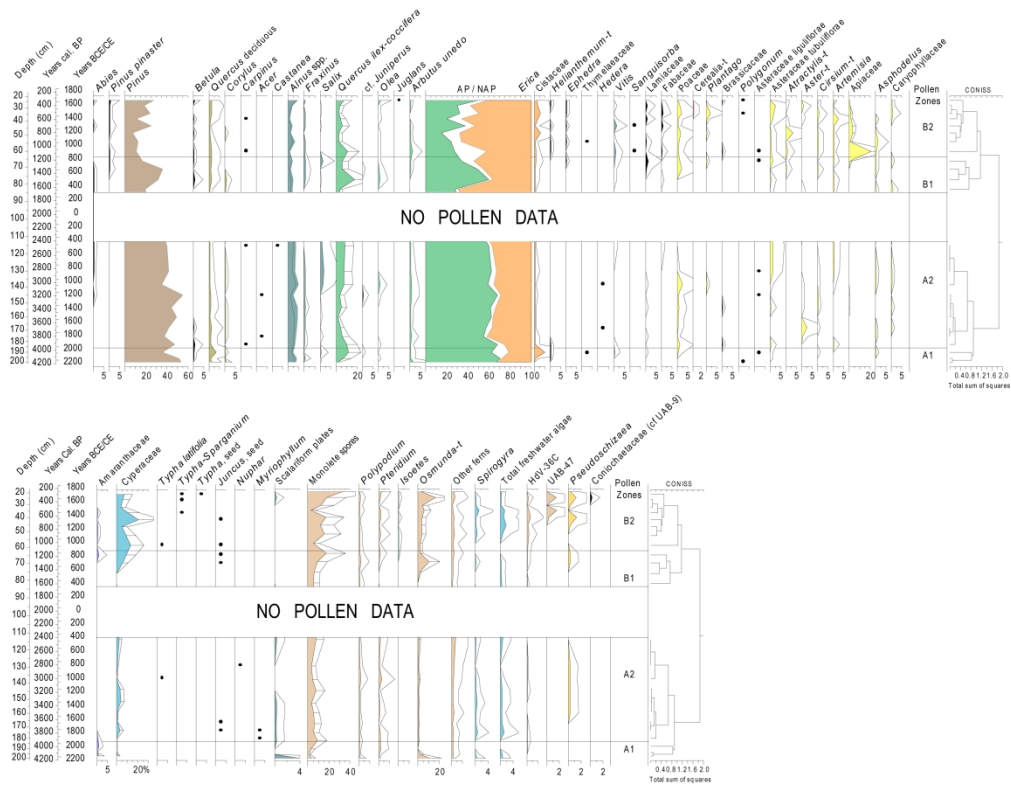


Figure 9 : Pollen and NPP percentage diagrams for Fangu core. White curves with depth bars show exaggerated curves x2; white curves, exaggeration x5; dots represent occurrences of <1%.

287x222mm (300 x 300 DPI)

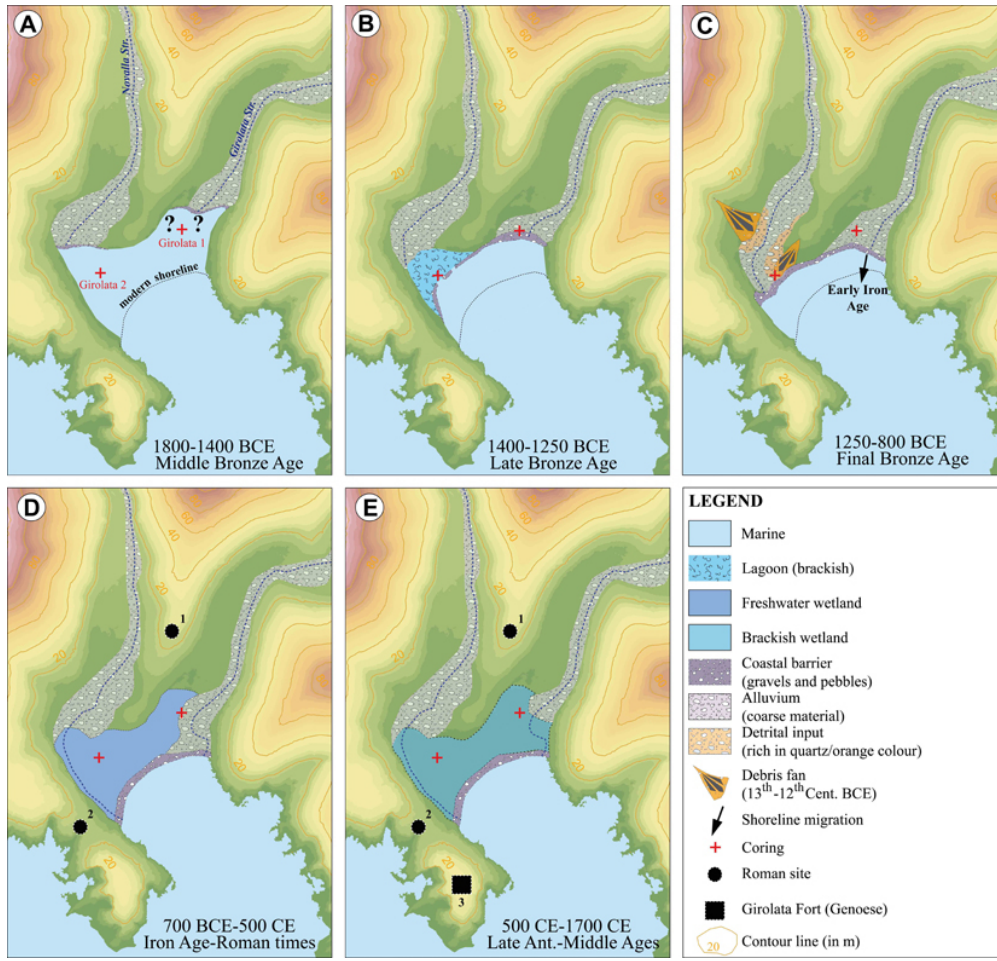


Figure 10 : Palaeogeographic reconstruction for the Girolata coastal plain for the last four millennia.

600x571mm (35 x 35 DPI)

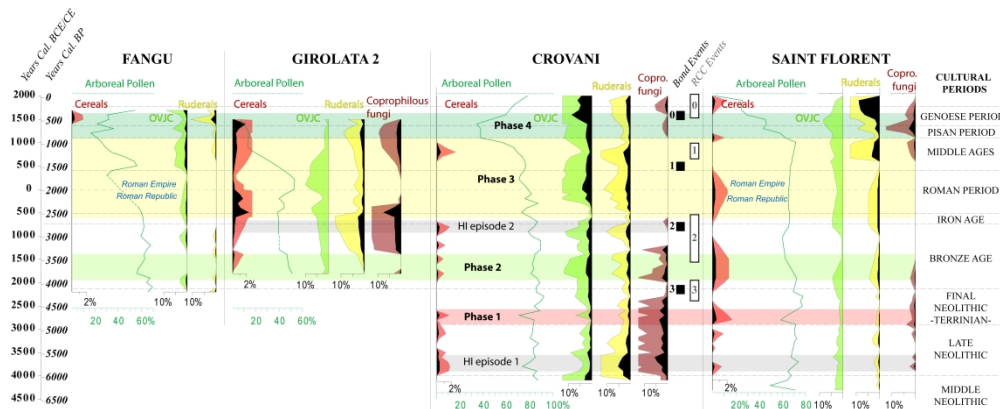


Figure 11 : Diagram showing the evolution of arboreal pollen and anthropogenic indicators in Fangu, Girolata 2, Crovani and Saint Florent cores for the last six millennia. Chronology of the cultural periods for Prehistory and Protohistory is derived from Tramoni and D'Anna (2016). Categories: OVJC (Olea, Vitis, Juglans, Castanea), Ruderals (Rumex, Brassicaceae, Polygonum, Plantago, Urtica), Coprophilous fungi (Sordaria-t, Sporormiella, Cercophora-t, Podospora-t, Delitschia). Colour frames indicate the four main phases of forest decline and grey frames indicate episodes of human impact without clear forest decline. Bond events (Bond et al., 1997) and RCC events (Mayewski et al., 2004) are reported on the graph.

386x156mm (300 x 300 DPI)

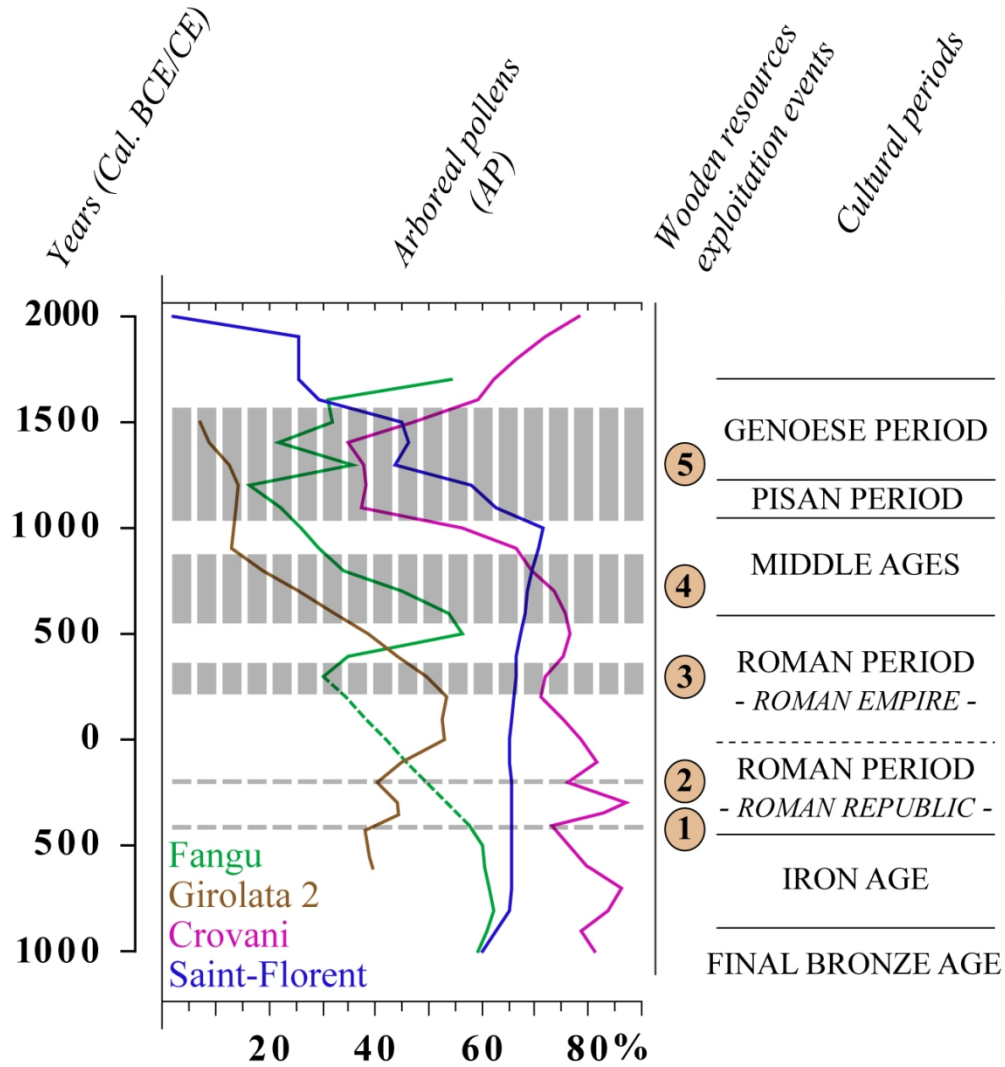


Figure 12 : Arboreal pollen (AP) evolution from the Iron Age onwards according to chronocultural periods for the sites of Saint-Florent (Nebbiu) ; Crovani (Balagne) ; Fangu and Girolata (Filosorma). The five major forest declines identified with palynology are highlighted with dashed grey bands; Event 2 alone is not documented in any known literary source. In the locator map : SF : Saint-Florent ; Cr. : Crovani ; Fa. : Fangu ; Gi. : Girolata ; Sa. : Sagone.

112x120mm (300 x 300 DPI)